

*Characterization of Reactive Tracers
for C-Wells Field Experiments I:
Electrostatic Sorption Mechanism, Lithium*

HYDROLOGY DOCUMENT NUMBER 585

Los Alamos

*Los Alamos National Laboratory is operated by the University of California for
the United States Department of Energy under contract W-7405-ENG-36.*

Prepared by S. M. Gonzales, Group HSE-12

This work was supported by the Yucca Mountain Project Office as part of the Civilian Radioactive Waste Management Program. This Project is managed by the U.S. Department of Energy, Nevada Operations Office.

An Affirmative Action/Equal Opportunity Employer

This report was prepared as an account of work sponsored by an agency of the United States Government. Neither the United States Government nor any agency thereof, nor any of their employees, makes any warranty, express or implied, or assumes any legal liability or responsibility for the accuracy, completeness, or usefulness of any information, apparatus, product, or process disclosed, or represents that its use would not infringe privately owned rights. Reference herein to any specific commercial product, process, or service by trade name, trademark, manufacturer, or otherwise, does not necessarily constitute or imply its endorsement, recommendation, or favoring by the United States Government or any agency thereof. The views and opinions of authors expressed herein do not necessarily state or reflect those of the United States Government or any agency thereof.

*Characterization of Reactive Tracers
for C-Wells Field Experiments I:
Electrostatic Sorption Mechanism, Lithium*

H. R. Fuentes

W. L. Polzer

E. H. Essington

B. D. Newman

CONTENTS

LIST OF FIGURES.	vi
LIST OF TABLES	viii
ABSTRACT	1
1.0 INTRODUCTION	2
2.0 TRACER SELECTION CRITERIA.	5
3.0 LITHIUM.	6
4.0 MATERIALS AND METHODS.	13
4.1 Prow Pass Samples and J-13 Water.	13
4.2 Procedures.	18
4.2.1 Adsorption Kinetics.	18
4.2.2 Desorption Kinetics.	20
4.2.3 Equilibrium Adsorption	21
4.2.4 Equilibrium Desorption	21
4.2.5 Potentiometric Titration	21
4.2.6 Electrophoresis.	22
4.2.7 Abrasion Effects	24
4.3 Models.	26
4.3.1 Isotherms.	26
4.3.2 Thermodynamics	30
4.4 Pre-experimental Geochemical Modeling	34
5.0 RESULTS AND DISCUSSION	37
5.1 Kinetics Experiments.	37
5.2 Equilibrium	38
5.2.1 Sorption Calculations.	38
5.2.2 Isotherm Evaluation.	40
5.2.3 Thermodynamic Parameter Estimation	50
5.2.4 Desorption	60
5.3 Potentiometric Studies.	63
6.0 SUMMARY AND CONCLUSIONS.	71
ACKNOWLEDGMENTS.	74
REFERENCES	76
APPENDIX A. ANALYTICAL INSTRUMENTATION.	81
APPENDIX B. ESTIMATES OF LITHIUM ADSORPTION AND DESORPTION EQUI- LIBRIUM CONCENTRATIONS.	85
APPENDIX C. EQUILIBRIUM CONCENTRATIONS AND MODELING VARIABLES	95
APPENDIX D. STATISTICAL AND MODEL PARAMETER ESTIMATES FOR ISOTHERMS .	113

LIST OF FIGURES

- Figure 1. Observed and predicted adsorption of lithium on a Prow Pass suspension in J-13 well water at 25°C for an initial concentration range of 1 to 2000 $\mu\text{g Li mL}^{-1}$ and a solid-to-liquid ratio of 1:20. Adsorbed lithium is determined in two ways: (1) based on measured lithium in solution (Li) and (2) based on a combination of measured lithium and other cations in solution (best estimate). Predicted lithium is based on the Modified Freundlich isotherm. 41
- Figure 2. Observed and predicted adsorption of lithium on a Prow Pass suspension in J-13 well water at 38°C for an initial concentration range of 1 to 2000 $\mu\text{g Li mL}^{-1}$ and a solid-to-liquid ratio of 1:20. Adsorbed lithium is determined in two ways: (1) based on measured lithium in solution (Li) and (2) based on a combination of measured lithium and other cations in solution (best estimate). Predicted lithium is based on the Modified Freundlich isotherm. 42
- Figure 3. Observed and predicted adsorption of lithium on a Prow Pass suspension in J-13 well water at 45°C for an initial concentration range of 1 to 2000 $\mu\text{g Li mL}^{-1}$ and a solid-to-liquid ratio of 1:20. Adsorbed lithium is determined in two ways: (1) based on measured lithium in solution (Li) and (2) based on a combination of measured lithium and other cations in solution (best estimate). Predicted lithium is based on the Modified Freundlich isotherm. 43
- Figure 4. Observed and predicted adsorption of lithium on a Prow Pass suspension in J-13 well water at 25°C for an initial concentration range of 1 to 150 $\mu\text{g Li mL}^{-1}$ and a solid-to-liquid ratio of 1:10. Adsorbed lithium is determined in two ways: (1) based on measured lithium in solution (Li) and (2) based on a combination of measured lithium and other cations in solution (best estimate). Predicted lithium is based on the Modified Freundlich isotherm 44
- Figure 5. Observed and predicted adsorption of lithium on a Prow Pass suspension in J-13 well water at 38°C for an initial concentration range of 1 to 150 $\mu\text{g Li mL}^{-1}$ and a solid-to-liquid ratio of 1:10. Adsorbed lithium is determined in two ways: (1) based on measured lithium in solution (Li) and (2) based on a combination of measured lithium and other cations in solution (best estimate). Predicted lithium is based on the Modified Freundlich isotherm. 45

Figure 6.	Observed and predicted adsorption of lithium on a Prow Pass suspension in J-13 well water at 45 ⁰ C for an initial concentration range of 1 to 150 $\mu\text{g Li mL}^{-1}$ and a solid-to-liquid ratio of 1:10. Adsorbed lithium is determined in two ways: (1) based on measured lithium in solution (Li) and (2) based on a combination of measured lithium and other cations in solution (best estimate). Predicted lithium is based on the Modified Freundlich isotherm.	46
Figure 7.	Observed and predicted adsorption and desorption of lithium on a Prow Pass suspension in J-13 well water at 38 ⁰ C for an initial concentration range of 1 to 2000 $\mu\text{g Li mL}^{-1}$ and a solid-to-liquid ratio of 1:20. Predicted lithium is based on the Modified Freundlich isotherm	64
Figure 8.	Observed and predicted adsorption and desorption of lithium on a Prow Pass suspension in J-13 well water at 38 ⁰ C for an initial concentration range of 1 to 150 $\mu\text{g Li mL}^{-1}$ and a solid-to-liquid ratio of 1:10. Predicted lithium is based on the Modified Freundlich isotherm	65
Figure 9.	Potentiometric titration of Prow Pass in suspension with J-13 well water and NaClO_4 electrolyte at 38 ⁰ C without the addition of lithium.	67
Figure 10.	Potentiometric titration of Prow Pass in suspension with J-13 well water and NaClO_4 electrolyte at 38 ⁰ C with the addition of 900 $\mu\text{g Li mL}^{-1}$	68
Figure 11.	Electrophoretic behavior of a colloidal suspension of Prow Pass in J-13 well water and NaClO_4 electrolyte at 38 ⁰ C with the addition of 900 $\mu\text{g Li mL}^{-1}$	69
Figure 12.	Electrophoretic behavior of a colloidal suspension of Prow Pass in J-13 well water and NaClO_4 electrolyte at 38 ⁰ C without the addition of lithium.	70

LIST OF TABLES

I.	GENERIC CLASSIFICATION OF ADSORPTION PROCESSES.	3
II.	LITHIUM CHARACTERISTICS	7
III.	LITHIUM BROMIDE CHARACTERISTICS	8
IV.	J-13 WATER BEFORE AND AFTER EQUILIBRATION WITH PROV PASS MATERIALS ($\mu\text{g mL}^{-1}$)	15
V.	PHYSICOCHEMICAL CHARACTERIZATION OF PROV PASS TUFF SAMPLES (<500 μm) USED IN THE INVESTIGATIONS.	16
VI.	REGRESSION AND COMPARISON BETWEEN SIZE DISTRIBUTIONS BEFORE AND AFTER TUMBLING.	25
VII.	PREDICTIONS FOR LITHIUM DISTRIBUTION IN PROV PASS AND J-13 WATER ADSORPTION EXPERIMENTS AT 38 ^o C ($\text{Li} = 2000 \mu\text{g mL}^{-1}$ AS LiBr).	36
VIII.	A COMPARISON OF ESTIMATED PARAMETERS OF FOUR ISOTHERM MODELS FOR THE ADSORPTION OF LITHIUM ON A PROV PASS SUSPENSION IN J-13 WELL WATER FOR AN INITIAL CONCENTRATION RANGE OF 1 TO 2000 $\mu\text{g Li mL}^{-1}$ AND A SOLID-TO-LIQUID RATIO OF 1:20	48
IX.	A COMPARISON OF ESTIMATED PARAMETERS OF FOUR ISOTHERM MODELS FOR THE ADSORPTION OF LITHIUM ON A PROV PASS SUSPENSION IN J-13 WELL WATER FOR AN INITIAL CONCENTRATION RANGE OF 1 TO 150 $\mu\text{g Li mL}^{-1}$ AND A SOLID-TO-LIQUID RATIO OF 1:10.	51
X.	PARAMETER VALUES FOR THE ESTIMATION OF A THERMODYNAMIC EQUILIBRIUM CONSTANT FOR THE LITHIUM ADSORPTION ON A PROV PASS SUSPENSION IN J-13 WELL WATER AT THREE TEMPERATURES FOR THE INITIAL CONCENTRATION RANGE OF 1 TO 2000 $\mu\text{g Li mL}^{-1}$ AND A SOLID-TO-LIQUID RATIO OF 1:20	54
XI.	THERMODYNAMIC CONSTANTS ESTIMATED FOR LITHIUM ADSORPTION ON A PROV PASS SUSPENSION IN J-13 WELL WATER AT THREE TEMPERATURES FOR AN INITIAL CONCENTRATION RANGE OF 1 TO 2000 $\mu\text{g Li mL}^{-1}$ AND A SOLID-TO-LIQUID RATIO OF 1:20	55
XII.	PARAMETER VALUES FOR THE ESTIMATION OF THERMODYNAMIC EQUILIBRIUM CONSTANTS FOR LITHIUM ADSORPTION ON A PROV PASS SUSPENSION IN J-13 WELL WATER AT 38 ^o C AND 45 ^o C FOR THE INITIAL CONCENTRATION RANGE OF 1 TO 150 $\mu\text{g Li mL}^{-1}$ AND A SOLID-TO-LIQUID RATIO OF 1:10.	57

XIII. THERMODYNAMIC CONSTANTS ESTIMATED FOR LITHIUM ADSORPTION ON A PROV PASS SUSPENSION IN J-13 WELL WATER AT 38⁰C AND 45⁰C FOR AN INITIAL CONCENTRATION RANGE OF 1 TO 150 $\mu\text{g Li mL}^{-1}$ AND A SOLID-TO-LIQUID RATIO OF 1:10 58

XIV. DATA USED IN THE CALCULATION OF EQUILIBRIUM CONSTANTS FOR THE ADSORPTION OF LITHIUM ON A PROV PASS SUSPENSION IN J-13 WELL WATER AT THREE TEMPERATURES FOR THE INITIAL CONCENTRATION RANGE OF 1 TO 150 $\mu\text{g Li mL}^{-1}$ AND A SOLID-TO-LIQUID RATIO OF 1:20. . . . 61

XV. EQUILIBRIUM CONSTANTS AND ENTHALPIES FOR THE ADSORPTION OF LITHIUM ON A PROV PASS SUSPENSION IN J-13 WELL WATER AT TEMPERATURES OF 25⁰C, 38⁰C, AND 45⁰C FOR THE INITIAL CONCENTRATION RANGE OF 1 TO 2000 $\mu\text{g Li mL}^{-1}$ AND A SOLID-TO-LIQUID RATIO OF 1:20. 62

B-I. ADSORBED LITHIUM CONCENTRATIONS AS ESTIMATED BY TWO METHODS AND THOSE CONSIDERED BEST ESTIMATES FOR ADSORPTION ON A PROV PASS SUSPENSION IN J-13 WELL WATER AT 25⁰C FOR AN INITIAL CONCENTRATION RANGE OF 1 TO 2000 $\mu\text{g Li mL}^{-1}$ AND A SOLID-TO-LIQUID RATIO OF 1:20 87

B-II. ADSORBED LITHIUM CONCENTRATIONS AS ESTIMATED BY TWO METHODS AND THOSE CONSIDERED BEST ESTIMATES FOR ADSORPTION ON A PROV PASS SUSPENSION IN J-13 WELL WATER AT 38⁰C FOR AN INITIAL CONCENTRATION RANGE OF 1 TO 2000 $\mu\text{g Li mL}^{-1}$ AND A SOLID-TO-LIQUID RATIO OF 1:20 88

B-III. ADSORBED LITHIUM CONCENTRATIONS AS ESTIMATED BY TWO METHODS AND THOSE CONSIDERED BEST ESTIMATES FOR ADSORPTION ON A PROV PASS SUSPENSION IN J-13 WELL WATER AT 45⁰C FOR AN INITIAL CONCENTRATION RANGE OF 1 TO 2000 $\mu\text{g Li mL}^{-1}$ AND A SOLID-TO-LIQUID RATIO OF 1:20 89

B-IV. ADSORBED LITHIUM CONCENTRATIONS AS ESTIMATED BY TWO METHODS AND THOSE CONSIDERED BEST ESTIMATES FOR ADSORPTION ON A PROV PASS SUSPENSION IN J-13 WELL WATER AT 25⁰C FOR AN INITIAL CONCENTRATION RANGE OF 1 TO 150 $\mu\text{g Li mL}^{-1}$ AND A SOLID-TO-LIQUID RATIO OF 1:10 90

B-V. ADSORBED LITHIUM CONCENTRATIONS AS ESTIMATED BY TWO METHODS AND THOSE CONSIDERED BEST ESTIMATES FOR ADSORPTION ON A PROV PASS SUSPENSION IN J-13 WELL WATER AT 38⁰C FOR AN INITIAL

	CONCENTRATION RANGE OF 1 TO 150 $\mu\text{g Li mL}^{-1}$ AND A SOLID-TO-LIQUID RATIO OF 1:10	91
B-VI.	ADSORBED LITHIUM CONCENTRATIONS AS ESTIMATED BY TWO METHODS AND THOSE CONSIDERED BEST ESTIMATES FOR ADSORPTION ON A PROW PASS SUSPENSION IN J-13 WELL WATER AT 45°C FOR AN INITIAL CONCENTRATION RANGE OF 1 TO 150 $\mu\text{g Li mL}^{-1}$ AND A SOLID-TO-LIQUID RATIO OF 1:10	92
B-VII.	THE BEST ESTIMATE OF ADSORBED LITHIUM AS DETERMINED BY TWO METHODS FOR THE DESORPTION OF LITHIUM FROM A PROW PASS SUSPENSION IN J-13 WELL WATER AT 38°C FOR AN INITIAL CONCENTRATION RANGE OF 1 TO 2000 $\mu\text{g Li mL}^{-1}$ AND A SOLID-TO-LIQUID RATIO OF 1:20	93
B-VIII.	THE BEST ESTIMATE OF ADSORBED LITHIUM AS DETERMINED BY TWO METHODS FOR THE DESORPTION OF LITHIUM FROM A PROW PASS SUSPENSION IN J-13 WELL WATER AT 38°C FOR AN INITIAL CONCENTRATION RANGE OF 1 TO 150 $\mu\text{g Li mL}^{-1}$ AND A SOLID-TO-LIQUID RATIO OF 1:10	94
C-I.	ADSORPTION EQUILIBRIUM DATA FOR THE 1-2000 $\mu\text{g mL}^{-1}$ RANGE OF INITIAL LITHIUM CONCENTRATIONS IN SOLUTION AT 25°C. CONCENTRATIONS CORRESPOND TO MEASURED LITHIUM; SOLID-TO-LIQUID RATIO = 1:20.	99
C-II.	ADSORPTION EQUILIBRIUM DATA FOR THE 1-2000 $\mu\text{g mL}^{-1}$ RANGE OF INITIAL LITHIUM CONCENTRATIONS IN SOLUTION AT 25°C. CONCENTRATIONS ARE BEST ESTIMATES FROM MEASURED LITHIUM AND OTHER CATIONS; SOLID-TO-LIQUID RATIO = 1:20	100
C-III.	ADSORPTION EQUILIBRIUM DATA FOR THE 1-2000 $\mu\text{g mL}^{-1}$ RANGE OF INITIAL LITHIUM CONCENTRATIONS IN SOLUTION AT 38°C. CONCENTRATIONS CORRESPOND TO MEASURED LITHIUM; SOLID-TO-LIQUID RATIO = 1:20.	101
C-IV.	ADSORPTION EQUILIBRIUM DATA FOR THE 1-2000 $\mu\text{g mL}^{-1}$ RANGE OF INITIAL LITHIUM CONCENTRATIONS IN SOLUTION AT 38°C. CONCENTRATIONS ARE BEST ESTIMATES FROM MEASURED LITHIUM AND OTHER CATIONS; SOLID-TO-LIQUID RATIO = 1:20	102

C-V.	ADSORPTION EQUILIBRIUM DATA FOR THE 1-2000 $\mu\text{g mL}^{-1}$ RANGE OF INITIAL LITHIUM CONCENTRATIONS IN SOLUTION AT 45°C. CONCENTRATIONS CORRESPOND TO MEASURED LITHIUM; SOLID-TO-LIQUID RATIO = 1:20.103
C-VI.	ADSORPTION EQUILIBRIUM DATA FOR THE 1-2000 $\mu\text{g mL}^{-1}$ RANGE OF INITIAL LITHIUM CONCENTRATIONS IN SOLUTION AT 45°C. CONCENTRATIONS ARE BEST ESTIMATES FROM MEASURED LITHIUM AND OTHER CATIONS; SOLID-TO-LIQUID RATIO = 1:20104
C-VII.	ADSORPTION EQUILIBRIUM DATA FOR THE 1-150 $\mu\text{g mL}^{-1}$ RANGE OF INITIAL LITHIUM CONCENTRATIONS IN SOLUTION AT 25°C. CONCENTRATIONS CORRESPOND TO MEASURED LITHIUM; SOLID-TO-LIQUID RATIO = 1:10.105
C-VIII.	ADSORPTION EQUILIBRIUM DATA FOR THE 1-150 $\mu\text{g mL}^{-1}$ RANGE OF INITIAL LITHIUM CONCENTRATIONS IN SOLUTION AT 25°C. CONCENTRATIONS ARE BEST ESTIMATES FROM MEASURED LITHIUM AND OTHER CATIONS; SOLID-TO-LIQUID RATIO = 1:10106
C-IX.	ADSORPTION EQUILIBRIUM DATA FOR THE 1-150 $\mu\text{g mL}^{-1}$ RANGE OF INITIAL LITHIUM CONCENTRATIONS IN SOLUTION AT 38°C. CONCENTRATIONS CORRESPOND TO MEASURED LITHIUM; SOLID-TO-LIQUID RATIO = 1:10.107
C-X.	ADSORPTION EQUILIBRIUM DATA FOR THE 1-150 $\mu\text{g mL}^{-1}$ RANGE OF INITIAL LITHIUM CONCENTRATIONS IN SOLUTION AT 38°C. CONCENTRATIONS ARE BEST ESTIMATES FROM MEASURED LITHIUM AND OTHER CATIONS; SOLID-TO-LIQUID RATIO = 1:10108
C-XI.	ADSORPTION EQUILIBRIUM DATA FOR THE 1-150 $\mu\text{g mL}^{-1}$ RANGE OF INITIAL LITHIUM CONCENTRATIONS IN SOLUTION AT 45°C. CONCENTRATIONS CORRESPOND TO MEASURED LITHIUM; SOLID-TO-LIQUID RATIO = 1:10.109
C-XII.	ADSORPTION EQUILIBRIUM DATA FOR THE 1-150 $\mu\text{g mL}^{-1}$ RANGE OF INITIAL LITHIUM CONCENTRATIONS IN SOLUTION AT 45°C. CONCENTRATIONS ARE BEST ESTIMATES FROM MEASURED LITHIUM AND OTHER CATIONS; SOLID-TO-LIQUID RATIO = 1:10110

C- XIII. DESORPTION EQUILIBRIUM DATA FOR THE 1-2000 $\mu\text{g mL}^{-1}$ RANGE OF INITIAL LITHIUM CONCENTRATIONS IN SOLUTION AT 38°C. CONCENTRATIONS ARE BEST ESTIMATES FROM MEASURED LITHIUM AND OTHER CATIONS; SOLID-TO-LIQUID RATIO = 1:20 111

D- I. STATISTICAL AND MODEL PARAMETER ESTIMATES OF THE LINEAR ISOTHERM FOR THE ADSORPTION OF LITHIUM ON A PROV PASS SUSPENSION IN J-13 WELL WATER FOR AN INITIAL LITHIUM CONCENTRATION RANGE OF 1 TO 2000 $\mu\text{g Li mL}^{-1}$ AND A SOLID-TO-LIQUID RATIO OF 1:20. 114

D- II. STATISTICAL AND MODEL PARAMETER ESTIMATIONS OF THE LANGMUIR ISOTHERM FOR THE ADSORPTION OF LITHIUM ON A PROV PASS SUSPENSION IN J-13 WELL WATER FOR AN INITIAL LITHIUM CONCENTRATION RANGE OF 1 TO 2000 $\mu\text{g Li mL}^{-1}$ AND A SOLID-TO-LIQUID RATIO OF 1:20. 115

D- III. STATISTICAL AND MODEL PARAMETER ESTIMATES OF THE FREUNDLICH ISOTHERM FOR THE ADSORPTION OF LITHIUM ON A PROV PASS SUSPENSION IN J-13 WELL WATER FOR AN INITIAL CONCENTRATION RANGE OF 1 TO 2000 $\mu\text{g Li mL}^{-1}$ AND A SOLID-TO-LIQUID RATIO OF 1:20 . . . 116

D- IV. STATISTICAL AND MODEL PARAMETER ESTIMATES OF THE MODIFIED FREUNDLICH ISOTHERM FOR THE ADSORPTION OF LITHIUM ON A PROV PASS SUSPENSION IN J-13 WELL WATER FOR AN INITIAL CONCENTRATION RANGE OF 1 TO 2000 $\mu\text{g Li mL}^{-1}$ AND A SOLID-TO-LIQUID RATIO OF 1:20 117

D- V. STATISTICAL AND MODEL PARAMETER ESTIMATES OF THE LINEAR ISOTHERM FOR THE ADSORPTION OF LITHIUM ON A PROV PASS SUSPENSION IN J-13 WELL WATER FOR AN INITIAL CONCENTRATION RANGE OF 1 TO 150 $\mu\text{g Li mL}^{-1}$ AND A SOLID-TO-LIQUID RATIO OF 1:10. 118

D- VI. STATISTICAL AND MODEL PARAMETER ESTIMATES OF THE LANGMUIR ISOTHERM FOR THE ADSORPTION OF LITHIUM ON A PROV PASS SUSPENSION IN J-13 WELL WATER FOR AN INITIAL CONCENTRATION RANGE OF 1 TO 150 $\mu\text{g Li mL}^{-1}$ AND A SOLID-TO-LIQUID RATIO OF 1:10 119

D- VII. STATISTICAL AND MODEL PARAMETER ESTIMATES OF THE FREUNDLICH ISOTHERM FOR THE ADSORPTION OF LITHIUM ON A PROV PASS SUSPENSION IN J-13 WELL WATER FOR AN INITIAL CONCENTRATION RANGE OF 1 TO 150 $\mu\text{g Li mL}^{-1}$ AND A SOLID-TO-LIQUID RATIO OF 1:10 120

D- VIII. STATISTICAL AND MODEL PARAMETER ESTIMATES OF THE MODIFIED FREUNDLICH ISOTHERM FOR THE ADSORPTION OF LITHIUM ON A PROV

PASS SUSPENSION IN J-13 WELL WATER FOR AN INITIAL CONCEN-
TRATION RANGE OF 1 TO 150 $\mu\text{g Li mL}^{-1}$ AND A SOLID-TO-LIQUID
RATIO OF 1:10121

CHARACTERIZATION OF REACTIVE TRACERS FOR C-WELLS FIELD EXPERIMENTS I: ELECTROSTATIC SORPTION MECHANISM, LITHIUM

by

H. R. Fuentes, W. L. Polzer, E. H. Essington,
and B. D. Newman

ABSTRACT

Lithium (Li^+) was introduced as lithium bromide (LiBr), as a retarded tracer for experiments in the C-wells complex at Yucca Mountain, Nevada Test Site, Nevada. The objective was to evaluate the potential of lithium to sorb predominately by physical forces. Lithium was selected as a candidate tracer on the basis of high solubility, good chemical and biological stability, and relatively low sorptivity; lack of bioaccumulation and exclusion as a priority pollutant in pertinent federal environmental regulations; good analytical detectability and low natural background concentrations; and a low cost. Laboratory experiments were performed with suspensions of Prow Pass cuttings from drill hole UE-25p#1 at depths between 549 and 594 m in J-13 water at a pH of

approximately 8 and in the temperature range of 25°C to 45°C . Batch equilibrium and kinetics experiments were performed; estimated thermodynamic constants, relative behavior between adsorption and desorption, and potentiometric studies provided information to infer the physical nature of lithium sorption.

Modeling of the equilibrium adsorption data indicates that lithium adsorption can be effectively represented in the range of 1 to $2000 \mu\text{g mL}^{-1}$ of initial lithium concentrations by the following isotherms: Linear, Langmuir, Freundlich, and Modified Freundlich. The Modified Freundlich is a general equation from which the others can be derived. The applicability of these isotherms to various flow regimes and influent conditions must be verified in laboratory column and field experiments.

Thermodynamic estimates indicate that lithium adsorbs to the Prow Pass in contact with J-13 water by a physical (electrostatic) mechanism. Enthalpies of adsorption are in the range expected for physical adsorption ($<12 \text{ kcal mole}^{-1}$). These results are supported by the reversibility between the adsorption and desorption of lithium and by its behavior in potentiometric studies. The potentiometric studies indicate that lithium did not cause a shift in the zero point of charge, which is indicative of physical sorption.

The characteristics of lithium in combination with the analysis of the laboratory batch equilibrium experiments

indicate that lithium is a good candidate tracer for a field test because it is expected to be only slightly retarded (a retardation factor of about 2) and to exhibit reversibility, a characteristic that should permit a better tracer recovery within a reasonable period of time, depending on the design of the field test. An advantage of adding Li^+ as LiBr is the simultaneous application of bromide, which is expected to behave as a conservative tracer for flow characterization.

1.0 INTRODUCTION

This report is part of the laboratory investigations conducted by Los Alamos National Laboratory (Los Alamos) as part of a study of Reactive Tracer Experiments in the C-wells and other wells in the Yucca Mountain Vicinity, Nevada. This study will provide information required by the Yucca Mountain Project (YMP) to describe the saturated-zone hydrologic characteristics at Yucca Mountain. The information is also required by the YMP geochemistry test program to evaluate the applicability of laboratory data to field conditions.

Laboratory investigations are being conducted to identify and characterize a group of tracers to be used in the C-wells field experiments at Yucca Mountain. Ideally, each tracer should adsorb by one predominant sorption mechanism, but various sorption mechanisms can actually occur simultaneously (for example, ion exchange and molecular sieve in zeolites) or sequentially (for example, film diffusion followed by ion exchange).

For this study two broad classes of sorption--physical and chemical--have been defined (1) and are described in Table I. Physical adsorption is very rapid (if not limited by diffusion rates), reversible, non-site-specific, and with low heats of adsorption ($<12 \text{ kcal mole}^{-1}$) (2). In contrast, chemisorption is more site-specific and results in adsorption energies similar to that of chemical bonding ($>20 \text{ kcal mole}^{-1}$) (2). Within these two general classes of adsorption, two major overall mechanisms are of concern in these

TABLE I
GENERIC CLASSIFICATION OF ADSORPTION PROCESSES

Characteristic	Process		
	Physical	Chemical	Intermediate
Enthalpy, ΔH (kcal mole ⁻¹)	Low <12	High >20	Low (?)
Changes in vibration frequency	Small (~0.1%)	Large	Small to large
Bond strength	Weak; easily reversible	Strong; partially or fully irrevers- ible	Weak; easily reversible
Type of bond	Nonspecific and reversible	Specific and reversible	Similar to physical and chemical
Forces	Too weak to cause physical or chemical change	Strong enough to cause physical and chemical change	Similar to physical and chemical change

Sources: References 1, 2.

investigations: electrostatic and chemical. Electrostatic adsorption represents a physical adsorption where ions in solution migrate to a diffuse layer (3,4) because of electrostatic attraction of ions to a surface of opposite charge and because of the dispersive influence of diffusion forces. Ion-exchange behavior is included in this definition if it is stoichiometric and reversible. Chemisorption refers to those cases where forces as large as those of chemical bonds hold the adsorbate (solute) to a site surface (3,4).

The sorption mechanism of a tracer can be inferred by several kinds of data: enthalpy and zero point of charge (ZPC). The enthalpy of sorption can be determined from isotherm data obtained at three temperatures. Enthalpy values of $<12 \text{ kcal mole}^{-1}$ are indicative of physical (electrostatic) sorption and those of $>20 \text{ kcal mole}^{-1}$ are indicative of chemical sorption. The ZPC can be determined from potentiometric titrations of electrolyte solutions in contact with the sorbent material and from electrophoretic measurements. If the presence of the tracer displaces the ZPC, then chemical sorption is indicated; if the ZPC is not displaced, then physical sorption is indicated.

The objective of the laboratory efforts is to characterize lithium (Li), introduced as lithium bromide (LiBr), as a candidate tracer of the electrostatic sorption mechanism for the field experiments. Laboratory batch experiments were conducted to evaluate and to model the extent of lithium adsorption to prepared samples from the Prow Pass Member of Yucca Mountain in J-13 well water (groundwater from the Yucca Mountain vicinity used as reference water in most geochemical investigations) by isotherms. In an attempt to demonstrate the physical nature of the adsorption of lithium, additional tests, including desorption in solutions of different ionic strengths and potentiometric studies, were conducted.

2.0 TRACER SELECTION CRITERIA

The selection of a tracer that adsorbs predominantly by physical adsorption was based on the following criteria:

- physicochemical properties,
- environmental regulations,
- detection, and
- cost.

The most important physical property is the reaction of the tracer with the rock matrix. However, the tracer should be sufficiently mobile to travel from the injection well to the observation wells in a reasonable period of time with reasonable groundwater flow rates. Thus, conventional tracers (5) that migrate with groundwater velocities are not adequate. On the other hand, the tracer must be stable so that other processes (for example, microbial uptake, complexation, and volatilization) do not complicate the monitoring, measuring, and modeling of the tracer. One criterion for the selection of tracers is obtaining approval from environmental agencies (federal, state, and local). Thus, chemicals included in major regulatory actions and their amendments have not been considered. Organic compounds with significant volatility and potential for complexation and compounds subject to biotransformation have also been excluded. These constraints leave limited choices. Radioactive tracers that offer advantages, for example, simpler analysis and more realistic simulation of repository releases, have been excluded from consideration for field tests because of their potential rejection by regulatory agencies.

3.0 LITHIUM

Literature searches and consultations with experts indicate that lithium as LiBr may satisfy most of the requirements discussed in Section 2.0. Tables II and III contain information on lithium and lithium bromide. This information includes physicochemical, thermodynamic, and toxicological characteristics, as well as references to the more pertinent federal environmental regulations. Lithium bromide dissolves and speciates into Li^+ and Br^- in water, thus producing two tracers, one reactive (nonconservative) and one nonreactive (conservative). LiBr is soluble in water at sufficiently high concentrations for easy use in field tests (i.e., hundreds of $\mu\text{g mL}^{-1}$). Lithium does not appear to form complexes that can complicate its chemistry and analytical identification. Additionally, its low potential for microbial conversion increases its traceability in laboratory and field studies.

As in the case of the rest of the alkali elements, lithium has a single electron in the outermost energy level of its atom. This electron, which is easily detachable, causes an extremely reactive chemical character. Because of the small size of its atom and ion, the behavior of lithium is transitional between the behavior of the alkali metals and that of the alkaline earth metals. These groups present a high ionic potential (ratio of ion radius to ion charge), which implies that lithium is expected to be highly soluble and more easily weatherable (leachable) than transition metals, aluminum cations, and oxyanions (15).

General information on lithium is available from a number of sources. Thermodynamic data include enthalpy, entropy, and free energy of formations for lithium and lithium species (16, 17, 18). Information on the distribution of lithium in the lithosphere and in specific geochemical systems has also been documented (19, 20).

TABLE II
LITHIUM CHARACTERISTICS

Physicochemical

Atomic number	3
Atomic weight	6.941
Specific gravity	0.53 at 20°C (solid)
Hydrated radius	3.4 Å
Ionic radius	0.68 Å
Heat of solution	-17,500 cal g ⁻¹
Natural isotopes	6 (7.4% abundance), 7 (92.6% abundance)

Thermodynamic (Li⁺)

$$\Delta G_f^\circ = -70.1 \text{ kcal mole}^{-1} \text{ at } 298.15\text{K}$$

$$\Delta H_f^\circ = -66.6 \text{ kcal mole}^{-1} \text{ at } 298.15\text{K}$$

$$S^\circ = 3.2 \text{ cal deg}^{-1} \text{ mole}^{-1} \text{ at } 298.15\text{K}$$

Toxicity

- The lithium ion may injure kidneys, especially if sodium intake is limited.
- Effect of low concentrations on aquatic life is unknown.
- Waterfowl toxicity data: not available.
- Food chain concentration potential: none.
- CAS RN: 74 39-93-2, NIOSH No: OJ 5540000

Environmental Regulations

Lithium is not included in the Clean Water Act, the Resource Conservation and Recovery Act, the Superfund Amendments Reauthorization Act or the Safe Drinking Water Act. It is inventoried in the Toxic Substances Control Act.

Sources: References 6, 7, 8, 9, 10, 11, 12

TABLE III
LITHIUM BROMIDE CHARACTERISTICS

Physicochemical

Form	White hygroscopic granular powder
Molecular weight	86.85
Melting point	550°C
Boiling point	1265°C
Specific gravity	3.464 at 25°C
Solubility in 100 g water	177 g at 20°C 202 g at 40°C 224 g at 60°C
Heat of solution	11.4 cal mole ⁻¹ (water)
Hydration states	Mono, di, tri and penta hydrate
Six-fold coordination	Bond length: 2.75 Angstrom

Thermodynamic

$$\Delta G_f^0 = -94.95 \text{ kcal mole}^{-1} \text{ at } 298.15\text{K}$$

$$\Delta H_f^0 = -95.61 \text{ kcal mole}^{-1} \text{ at } 298.15\text{K}$$

$$S^0 = 22.9 \text{ cal mole}^{-1} \text{ at } 298.15\text{K}$$

Toxicity

- LD₅₀ = 1,680 mg kg⁻¹ (tests with mice, subcutaneous)
- Large doses may cause CNS (central nervous system) depression. Chronic adsorption may cause skin eruptions and CNS disturbances because of bromide. May also cause disturbed blood electrolyte balance.
- CAS RN: 75 50-35-8; NIOSH No: OJ 5755000

Environmental Regulations

Lithium bromide is not included in the Clean Water Act, the Resource Conservation and Recovery Act, the Superfund Amendments and Reauthorization Act (lithium chromate, lithium hydride and bromine are included), or the Safe Drinking Water Act. It is inventoried in the Toxic Substances Control Act.

Sources: References 6, 9, 10, 11, 12, 13, 14

Sorption information for lithium on soils and rocks is scarce. A survey of the literature indicates a lack of pertinent investigations. The survey used computer searches to inventory journals in the fields of environmental science or engineering, soil chemistry, and geochemistry. This lack of success may be because lithium is not an element of concern in agricultural production and is not considered a contaminant according to environmental regulations. Two references (21, 22) deserve mention because they constitute recent summaries on the sorption of inorganic elements by materials of the subsurface environment. The first summary (21) reviewed literature from approximately 500 papers on cation exchange in soil systems. Selectivity coefficients and estimated thermodynamic parameters were compiled for soils and soil components in well-defined systems. Lithium was reported only as the resident cation of Li-clays in exchanges with alkali and ammonium ions NH_4^+ in solutions. The estimates of the excess free energy indicate that the exchange favors the adsorption of all the ions over lithium. A second recent bibliography was completed by the Energy Power Research Institute (EPRI) (22). This bibliography contained over 350 references, published before February 1983, dealing with chemical and biological attenuation mechanisms for 21 inorganic elements; lithium was not included. This survey found that adequate data exist to make quantitative estimates for only a few solutes and that attenuation is expected to vary as a function of the chemical element and the composition of the subsurface media. The above limited information on lithium illustrates its lack of priority in sorption research.

Most available basic information on the adsorption of lithium by natural adsorbents refers to its inclusion in studies to characterize differences of behavior among ions. Investigations as early as 1922 showed low exchange of lithium for barium and calcium in soils and high exchange of lithium for ions

with atomic weights higher than those of barium and calcium (23). Later investigations (24) examined the influence of solution concentration and the nature of the interacting ions on lithium adsorption. Selectivity sequences are used to document the effects of ion characteristics or behavior on adsorption preference of ions for an adsorbent. Such sequences included valence, equivalent volume, polarizability, interactions with resident ions, and complex formation.

Adsorption of lithium does not seem to involve a strong surface interaction. For instance, some studies strongly suggest that lithium shows a lower preference for natural ion exchangers than do the rest of alkali cations, namely, sodium (Na^+), potassium (K^+), rubidium (Rb^+), and cesium (Cs^+)(25). Helfferich (26) reported that exchangers show the lowest selectivity for lithium among most common cations. Other findings from investigations with soils and tuff report a low adsorption of lithium (27, 28). Low adsorption can be an advantage for a reactive tracer because it will result in lower retardation, which shortens breakthrough periods in field tests.

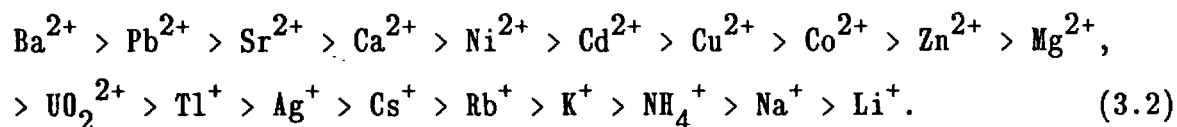
The general order of preference of monovalent cations by smectites (29) for the Group IA metal cations is



This sequence indicates a greater attraction of less hydrated cations to the interlayer of smectites. The less hydrated cations can more closely fit the cavity of the smectite six-membered tetrahedral rings. The sequence is explained at the molecular level (30) by the principle of hard and soft acids

and bases. Lithium is the hardest acid in the selectivity sequence, so it has less ability to exchange its solvent water molecules for the oxygen ions (soft base) in surface functional groups than do softer acids such as cesium.

A general selectivity sequence of most common cations by general-purpose cation exchangers is the following (26):



This selectivity shows lithium with the lowest preference. In addition, lithium is also the least strongly held cation on synthetic zeolites, compared with most of the other alkali elements and with alkaline earth elements.

Eisenman (25) developed the concept of "equivalent anion" to explain relative bonding strengths of cations in various types of exchangers. From the combination of cation size, cation charge, "equivalent anion," and hydration energies for the cations, predictions for the bonding energies of the alkali elements were made for natural exchangers. The predictions, expressed as free energies, compared fairly well with experimental measurements. The analysis predicts the bonding energies of all alkali ions to clays, zeolites, and feldspars. It predicts lithium to be the least adsorbed ion in the presence of sodium, potassium, cesium, or rubidium.

The limited current toxicological information for lithium bromide indicates that toxicity to aquatic life at low lithium concentrations has not been demonstrated and that bioaccumulation in food chains is not expected. The absence of regulatory concern in the major environmental acts suggests that the use of lithium as a tracer should be feasible. This feasibility

could be ensured by the use of low concentrations and by effective recovery of injected solutions. Of all the pertinent Federal acts, only the Toxic Substances Control Act (TSCA) includes lithium as part of an inventory. Lithium is not included in the 129 priority toxic pollutants (31). Although regulations do not specifically address lithium, it has been known to occur in groundwater, as reported by the Office of Technology Assessment (32). Critical to the constraints set by regulations is the consideration of groundwater quality standards defined by both State and local regulations in Nevada that may apply to the Yucca Mountain area. The role of State and local regulations is not discussed in this study.

Lithium in aqueous solutions can be determined by several conventional analytical techniques. Of these (33, 34), spectroscopy (e.g., atomic emission spectroscopy) and chromatography (e.g., ion chromatography) offer competitive analytical costs and low limits of detection. Limits of detection can be at least within the parts per billion range (ppb) but can be improved by concentration techniques. The background concentration of lithium in J-13 water is low (about $0.05 \mu\text{g mL}^{-1}$) compared with an operational range at least two orders of magnitude higher. The cost of lithium bromide is low enough not to be of any importance in tracer selection.

In summary, lithium as LiBr appears to be an excellent candidate tracer for hydrogeochemical investigations in Yucca Mountain because of its stability and weak adsorption. It may show enough adsorption to simulate the migration of weakly reactive tracers in the subsurface. This low degree of sorptivity has been demonstrated in intermediate-scale (caisson) experiments conducted with unsaturated and saturated Bandelier Tuff (28). Estimates for lithium retardation factors are slightly greater than one (up to about 1.3) when experimental breakthrough curves (within 6 m of traveling distance from the

source) are fitted to a one-dimensional advective-dispersive equation (28). Simultaneously, lithium may be more acceptable by regulatory agencies for use in groundwater studies than other tracers, is detectable in the $\mu\text{g L}^{-1}$ range by conventional analytical equipment, and is inexpensive. Currently available equipment allows adaptation to continuous-flow monitoring, which speeds up and improves the characterization of breakthrough profiles in the field.

4.0 MATERIALS AND METHODS

This section describes the Prow Pass samples and the J-13 well water used in all of the investigations. Information about experimental procedures and the application of geochemical modeling to experimental design is also presented in this section.

4.1 Prow Pass Samples and J-13 Water

Prow Pass material used in these experiments consisted of cuttings collected from drill hole UE-25p#1 about 630 m east of the C-wells complex. Fifteen sets of cuttings from depths between 1800 and 1950 feet (549 and 594 m) were selected because they represent the Prow Pass Member, which is the first geological barrier to radionuclide migration in the saturated zone (35). The general mineralogical composition of these samples is dominated by feldspars, quartz, and kaolinites, with small quantities of smectite, mica, and hematite (36). An analysis of a washed sample of cuttings (see next paragraph) showed larger percentages of feldspars, quartz, and cristobalite, with small quantities of smectite and hematite (37). This difference cannot be explained yet, but it may be related to variability of sampling. Compared with other cuttings from the drill holes in the C-wells area, these samples appeared to have the simplest mineralogic composition, helping to minimize

uncertainty in the laboratory but reducing the representativeness of the results for field projections.

The 15 samples of cuttings were washed with distilled water and composited to form sufficient material for the experiments. During drilling, the cuttings may have become contaminated with overlying rock materials and drilling material residues and additives that would interfere with the experiments. As much of the contaminating residue and additives as possible was removed by suspending the cuttings in distilled water and gently sonifying and decanting the fines after a period of settling. Thirty such treatments were necessary to remove the fine materials believed to contain the drilling contaminants.

The Prow Pass material was then ground with a ceramic pulverizer to pass a 500- μm stainless steel sieve. The ground material was conditioned with eight successive J-13 water washes; key chemical constituents of the washes were monitored for completeness of conditioning. Table IV summarizes the key constituents of the J-13 water as collected and after the first and eighth 24-h equilibrations with treated Prow Pass samples. Based on the limited change over the 8 days of treatment, it was concluded that pseudo-equilibrium had been reached within the first 24 h of contact time. The data from the eighth 24-h equilibration represent the background composition and are used as a reference for experiments with J-13 well water and Prow Pass materials.

The <500- μm sample was used in all the experiments. Characterization of the <500- μm fractions is given in Table V and includes specific surface area, ion exchange capacity, mineralogy by x-ray diffraction, and particle size classification.

Specific surface area was measured by three methods that gave different results, as shown in Table V. The Brunauer-Emmett-Teller (BET) method

TABLE IV
 J-13 WATER BEFORE AND AFTER EQUILIBRATION
 WITH PROV PASS MATERIALS ($\mu\text{g mL}^{-1}$)

Element	Original J-13 Water	First 24-h Equilibration	Eighth 24-h Equilibration	C-well ^a
Al	<0.03	0.47	0.25	--
B	0.13	0.13	0.13	--
Ba	<0.001	0.02	0.003	--
Ca	11.3	13.5	13.1	11
Fe	0.02	0.05	0.04	--
K	5	3	3.0	2
Li	0.040	0.09	0.05	0.11
Mg	<0.010	0.79	1.2	0.38
Mn	0.01	0.004	0.005	--
Na	44	50	42.0	55
Si	30	23	27.0	25
Sr	0.040	0.015	0.020	0.044
Cl	7	8	7	7
PO ₄	<2.5	<2.5	<2.5	--
SO ₄	19	23	19	22
HCO ₃	124	-- b	-- b	142
pH	7.2	-- b	-- b	7.8

^aSource: Reference 38.

^bNot analyzed.

TABLE V
 PHYSICOCHEMICAL CHARACTERIZATION OF PROW PASS
 TUFF SAMPLES (<500 μm) USED IN THE INVESTIGATIONS

Property	Measurement	
Specific Surface Area ($\text{m}^2 \text{g}^{-1}$):		
Quantachrome ^a , Brunauer-Emmett-Teller	3.46	
Microtrac	0.19 \pm 0.06	
Ethylene glycol monoethyl ether	0.26 \pm 0.12	
Cation exchange capacity (meq 100 g^{-1}):		
Na ⁺ acetate (pH 8.2)	16	
Exchangeable cations (meq 100 g^{-1}):		
	NH ₄ ⁺ acetate (pH 7.0)	Na ⁺ acetate (pH 8.2)
Ca ²⁺	14	7.2
Mg ²⁺	0.64	0.44
Na ⁺	4.2	—
K ⁺	1.1	1.8
Li ⁺	ND ^b	0.0068
X-ray diffraction (%):		
feldspar 60 \pm 7	quartz 22 \pm 2	
cristobalite 15 \pm 1	smectite 1 \pm 1	
hematite 1 \pm 1		
Particle size classification (%) ^c :		
sand 96	silt 4	clay <0.3

^aThis estimate was performed by Quantachrome Corporation (Syosset, NY) with a Quantasorb Jr.

^bND - Not detected.

^cU.S. Department of Agriculture classification scheme.

measures the amount of nitrogen gas required to complete a monolayer of nitrogen molecules absorbed by the exposed surface of the particle. The area was estimated to be $3.46 \text{ m}^2 \text{ g}^{-1}$. The ethylene glycol monoethyl ether (EGME) method, similar in principle to the BET method, gave results lower than those from the BET method ($0.26 \text{ m}^2 \text{ g}^{-1}$). This is understandable because the adsorbing component, EGME, is much larger than the nitrogen gas molecule and cannot penetrate the small pores accessible to nitrogen. The $0.19\text{-m}^2 \text{ g}^{-1}$ value obtained with the Leeds and Northrup Microtrac is lower than that of the EGME method although not significantly different, and is obtained during measurement of particle size distribution using laser-based light reflectance. The mean particle diameter of the ground samples was estimated by the Microtrac to be about $50 \mu\text{m}$. Assuming smooth spherical particles, the minimum specific surface area calculated for $50\text{-}\mu\text{m}$ particles at a density of 2.5 g cm^{-3} and 0.5 packing fraction is $0.05 \text{ m}^2 \text{ g}^{-1}$. The choice of the value of surface area to be used in calculations will be between 0.05 and $3.46 \text{ m}^2 \text{ g}^{-1}$ and will depend on the requirements of the specific computations.

Cation exchange capacity and exchangeable cations were measured on the Prow Pass materials with NH_4^+ (pH 7.0) and Na^+ (pH 8.2) as exchanging cations in an acetate buffer system. Exchangeable cations were recovered upon treating the NH_4^+ -saturated Prow Pass material with Na^+ acetate and the Na^+ -saturated Prow Pass with NH_4^+ acetate. Particle size classification of the prepared Prow Pass material was determined by sieve analysis for fractions greater than $44 \mu\text{m}$ and by a Micromeritics Sedigraph 5000D Particle Size Analyzer for the smaller fractions.

Water from well J-13, a natural groundwater, was the primary solution. This easily available water has been used as a standard water in sorption tasks for the Yucca Mountain Project (YMP). Synthetic waters are the choice

for development of fundamental information for individual minerals and tracers; however, natural groundwater was selected in an attempt to simulate field conditions more closely and to meet time and resource limitations. C-wells waters were considered but were not available for these investigations. The composition of the J-13 water is not greatly different from that of the C-wells water and thus should not affect results from these laboratory investigations. Key components of J-13 and C-wells waters are compared in Table IV. Before experimental use, the water was filtered to $<0.05 \mu\text{m}$ in order to remove potential colloidal particulates.

4.2 Procedures

Detailed procedures (DPs) have been formulated according to Los Alamos National Laboratory Quality Assurance Documents for the Yucca Mountain Project, No. 88, Volumes I, II, and III, 1988. These DPs describe sorption experiments, or activities supporting those experiments, that are being performed in the assessment of tracers for the C-wells project. These procedures were derived or modified from peer-reviewed published procedures. Appendix A describes instrumentation used in the investigations.

4.2.1 Adsorption Kinetics

Two types of kinetics studies were performed: batch tube studies to define minimum equilibration times; and controlled reactor studies to collect data for (a) evaluating the role of film transfer and internal diffusion in the laboratory experiments and (b) estimating activation energies.

The batch-tube method used 50-mL polyallomer centrifuge tubes with 2.0 g of Prow Pass material, which was conditioned by mixing for 24 h with 38 mL of J-13 water. After conditioning, 2 mL of tracer solution was added to each tube, and mixing and timing were started immediately. The filled tubes were

mixed continuously by tumbling in a modified Patterson-Kelley blender. Three replicates for each sampling time were maintained at a solid-to-liquid ratio of 1:20 and at a controlled temperature of 38°C ($\pm 2^{\circ}\text{C}$) for the duration of the experiment. The sampling times of 1 min, 0.5 h, 8 h, 24 h, 48 h, and 96 h were expected to cover the time necessary for the system to attain equilibrium.

Sampling involved centrifuging the tubes for 11 min at a relative centrifugal force (RCF) of 900 and then filtering the supernatant through a $0.45\text{-}\mu\text{m}$ syringe filter. The sample was then split into two 20-mL polyethylene vials. One vial was used for pH measurement and the other was acidified to 1% nitric acid, stored at 4°C , and chemically analyzed. During sampling of the first batch, bacteria growth was found in the tubes, so all subsequent experimental materials were sterilized in a steam autoclave before being used in the sorption experiments.

For the controlled reactor studies, ground and sieved Prow Pass material and J-13 water were added to a tared glass beaker to make the final solid-to-liquid ratio 1:20 or 1:10. The beaker and its contents were autoclaved and the contents were transferred to the controlled reactor vessel (a 500-mL glass kettle with baffles, a lid, and a mixing system with speed control). Other adsorption experiments with the controlled reactors were conducted at 25°C , 38°C , and 45°C , initial lithium solution concentrations of 15 and $75\ \mu\text{g mL}^{-1}$, and at mixing levels of 700, 1000, and 1500 rpm; these experiments extended over a period of 12 h with more samples withdrawn at the beginning than at the end. As with the previous experiments, equilibrium was reached within the first 2 h, confirming the adequacy of the 24-h standard equilibration time. The reactor and contents were allowed to condition for 24 h at constant mixing and a temperature of $38 \pm 2^{\circ}\text{C}$.

During mixing, an appropriate volume of tracer was added to the reactor; reaction timing started immediately. Samples were taken by withdrawing suspension from the reactor and filtering through a 0.45- μm syringe filter. Samples were acidified to 1% nitric acid, stored at 4⁰C, and chemically analyzed. The pH was measured on a sample withdrawn from the suspension before addition of the tracer and again after the last sample was taken.

4.2.2 Desorption Kinetics

Desorption kinetics was evaluated only for certain adsorption experimental conditions. The desorption method was basically the same for the batch tube and the controlled reactor studies; exceptions are noted below. J-13 water was used as the desorbing solution. Experimental conditions, for example, temperature, were maintained the same as in the adsorption step.

After the adsorption period in the batch tubes, the tracer solution was removed by centrifuging and decanting. The tubes were weighed and the amount of the entrained solution was determined. Samples of solution removed from the tubes were collected and analyzed to determine the amount of the entrained tracer. The solution phase in the controlled reactor was removed by vacuum filtration. The solids were washed twice with distilled water to remove much of the entrained nonsorbed tracer. A sample of the last wash was retained for pH and chemical analyses to determine the amount of tracer remaining in the reactor solution.

An amount of J-13 water was added to the tubes or to the reactor so that the solid-to-liquid ratio was maintained. Timing and mixing were started immediately after addition of the J-13 water.

Samples from the batch tubes were split as in the adsorption stage for pH and chemical analyses. Samples were collected from the controlled reactors in

the same manner as in the adsorption stage; pH was measured on the last sample collected. Sampling times were selected to monitor desorption kinetics for periods up to 48 h for the batch tubes and 96 h for the reactors.

4.2.3 Equilibrium Adsorption

Equilibrium experiments were performed at 25°C, 38°C, and 45°C, with up to ten initial tracer concentrations ranging from 1 to 2000 $\mu\text{g mL}^{-1}$. Section 4.2.1 describes the basic setup and the general procedure for both adsorption and desorption. The main difference between the kinetics and equilibrium experiments is that sampling in equilibrium experiments was only at the beginning and end of the equilibration period. The typical sampling time for equilibrium studies was 24 h after addition of the tracer.

4.2.4 Equilibrium Desorption

Desorption equilibrium was evaluated only for certain equilibrium conditions. J-13 water was used as the desorbing solution. Section 4.2.2 describes the setup and procedure followed for equilibrium desorption.

4.2.5 Potentiometric Titration

Prow Pass material was suspended in electrolyte solutions of 0.005 or 0.1 M NaClO_4 in a ratio of 2 g solids to 40 g electrolyte. A second series of samples was prepared in the same manner, but the electrolyte solutions contained 900 $\mu\text{g mL}^{-1}$ lithium as LiBr. Each sample was duplicated and the experiment was conducted at 38°C. To each sample a small amount of standardized 0.25 M HClO_4 or 0.25 M NaOH was added; treatments ranged from 0

to 3000 μL . The samples were mixed by tumbling for 6 h and were then centrifuged, and pH was measured directly on the clarified supernatant. Concurrently, a separate set of electrolyte samples was prepared similarly but without Prow Pass solids. The pH measurements on these samples were used as the reference in the following calculation to estimate the net adsorbed charge ($\mu\text{moles m}^{-2}$):

$$s_o = k(\Delta\text{H} - \Delta\text{OH}) \text{ or} \quad (4.1)$$

$$s_o = k([\text{H}]_a - [\text{OH}]_a - [\text{H}]_r + [\text{OH}]_r), \quad (4.2)$$

where

S_o = net adsorbed charge ($\mu\text{moles m}^{-2}$)

ΔH = the amount of the added H^+ consumed, $\mu\text{moles mL}^{-1}$,

ΔOH = the amount of the added OH^- consumed, $\mu\text{moles mL}^{-1}$,

$[\text{H}]_a$ = the concentration of protons remaining after reaction with the solid, $\mu\text{moles mL}^{-1}$,

$[\text{OH}]_a$ = the concentration of hydroxide remaining after reaction with the solid, $\mu\text{moles mL}^{-1}$,

$[\text{H}]_r$ = the concentration of protons remaining in the electrolyte not reacted with the solids, $\mu\text{moles mL}^{-1}$,

$[\text{OH}]_r$ = the concentration of hydroxide remaining in the electrolyte not reacted with the solids, $\mu\text{moles mL}^{-1}$, and

k = system constant, mL m^{-2} .

4.2.6 Electrophoresis

Electrophoresis refers to the movement of charged particles relative to a stationary solution in an applied potential. The pH at which a colloid is

electrokinetically uncharged is referred to as the zero point of charge (ZPC). If the ZPC is displaced by the addition of a tracer, then chemical sorption is indicated; if not, then physical sorption is indicated. Electrophoretic mobility of colloidal suspensions is used to determine the ZPC.

Electrophoretic mobility (EM) is a measure of the velocity of a colloid in response to an electric field and is defined as the colloid velocity in micrometers per second divided by the strength of the electrical field in volts per centimeter. An EM run consists of timing the migration of a number of particles over a measured distance under an applied voltage. Measurements of EM were made with a Zeta-Meter 3.0 System.

The samples used for EM were the same ones used in the potentiometric measurements, Section 4.2.5. The solids were resuspended in water and then allowed a minimum of 10 h to settle. A portion of the sample (e.g., 1 mL) that contained the desired particle size range (e.g., $<2 \mu\text{m}$) and proportion of solids was retrieved from the solution after 10 h and placed in a separate container. The remaining sample was then centrifuged at an RCF of 900 for approximately 10 min to separate the majority of the particles from the bulk liquid. The clarified liquid was then added to the 1 mL sample. This is essentially the method of reconstitution described by the manufacturer of the Zeta-Meter 3.0.

Four samples were prepared by vacuum filtration through filter paper with a pore diameter of $8 \mu\text{m}$. This method proved to be time consuming, however, and reconstitution was used for the remaining samples. EM results were obtained on either reconstituted or filtered duplicate suspensions in which EM values compared favorably: -2.578 with -2.563 and -2.641 with -2.743 $\mu\text{m cm per volt second}$.

4.2.7 Abrasion Effects

Tumbling (or stirring) suspensions (tube or reactor) of soils and geological samples may cause abrasion that could change the particle size distributions and create new sorption surfaces or active sites. The degree of abrasion of Prow Pass was evaluated by measurement of particle size distributions on mixed and nonmixed materials. Data for the average mesh sizes of 774 through 31 μm were applied to a model for particle size distribution (39) that was used to fit the equation

$$Y = 1 - \exp (x/x_0)^n , \quad (4.3)$$

where

Y = cumulative fraction of material by weight less than size x (x in μm),

x_0 = characteristic particle size, μm , and,

n = constant specific to the sample and breakage conditions.

Linearization of Equation (4.3) followed by linear regression provided a goodness of fit and an estimate of the constants. Table VI summarizes those estimates and regression statistics. An F-test comparison of the regression for the sample before tumbling and that after tumbling indicated that the two size distributions were significantly different at the 99.5% confidence level. Thus, reactor experiments may affect distribution of sizes, but further evaluation is needed to estimate the variability in tracer response relative to different particle size distributions.

TABLE VI
REGRESSION AND COMPARISON BETWEEN SIZE DISTRIBUTIONS
BEFORE AND AFTER TUMBLING

Statistics ^a	Sample before Tumbling	Sample after Tumbling
R^2	0.945	0.978
C.V.	36.400	65.370
n	2.190	1.749
x_0	194.98	186.21
F-test	F-calculated = 33.50 > F-tabulated (at 99.5% confidence level) = 6.27; then the distributions are significantly different.	

^a R^2 = index of determination; C.V. = coefficient of variance; n, x_0 = constants in Equation (4.3).

4.3 Models

Evaluation of the suitability of lithium as a tracer of physical sorption in field tests in the C-wells saturated zone included modeling with isotherm and thermodynamic models. The isotherm models were used to determine the extent of sorption and to provide information for the thermodynamic models. The thermodynamic models were used to estimate energies associated with the mechanism of sorption.

4.3.1 Isotherms

Isotherms have been derived and used to represent sorptive behavior in a variety of disciplines (2, 3, 40, 41). Three of the more commonly used isotherms are the Linear, Langmuir, and Freundlich. These three models plus the Modified Freundlich isotherm, a general isotherm from which the others can be derived, were fitted to the equilibrium lithium concentrations.

The simplest and most widely used of the equilibrium sorption isotherms is the linear relationship

$$S = K_d C , \tag{4.4}$$

where

S = concentration of solute sorbed by the solid,

C = concentration of solute in solution, and

K_d = distribution coefficient.

This expression is widely used in transport models to describe the sorption of reactive solutes by solids. One limitation is that the maximum quantity of adsorption is not included. The distribution coefficient K_d is

the ratio of retention of solute by the solid to the solute in solution and is assumed to be independent of concentration. This is not always the case, and conclusions drawn from modeling based on assumptions of linear sorption behavior may not be valid.

Langmuir developed a quantitative model that has also been widely applied to describe experimental data (42). The Langmuir equation was derived for the sorption of gases on a solid surface. Nevertheless, it has been extended to include the sorption of solutes by solids. The basic expression takes the form

$$S = \frac{kbC}{1 + kC} , \quad (4.5)$$

where

$k, b =$ empirical constants.

Linearization of Equation (4.5) provides the following transformation to be fitted to the experimental data:

$$C/S = (1/b)C + 1/kb. \quad (4.6)$$

In this expression, k is a measure of the strength of the sorption bond and b is the maximum amount of the solute that can be sorbed by the solid (40).

This isotherm is based on the theoretical assumption that the sorption sites are homogeneously distributed relative to energy potentials.

The Freundlich isotherm has the form

$$S = KC^N , \quad (4.7)$$

where

K, N = empirical constants.

Estimation of the constants is possible by the logarithmic transformation of Equation (4.7) to

$$\log S = N \log C + \log K. \quad (4.8)$$

This expression is also very popular in the literature because of the flexibility of the exponential function to fit experimental data. The equation is a better representation of heterogeneous behavior.

The Linear and Langmuir isotherms assume that the energy of adsorption is the same for all active sites on the adsorbent surface. However, the assumption fails in many cases because either pure mineral or multimineral adsorption sites interact with solutes at different energies (heterogeneity). These differences among site energies require the identification of those energy distributions that characterize the heterogeneity of a particular adsorbent/solute interaction. Then, equations such as the Freundlich isotherm are better modeling alternatives.

Sips (43) introduced and discussed an isotherm that suggests a Gaussian-like statistical function that could represent the distribution of site/solute interactions. This isotherm is based on the assumption that localized adsorption occurs without interaction among sites and was presented as an expansion of the conventional Freundlich isotherm. Sposito (44), following the derivation obtained by Sips (43) and using a Langmuir isotherm to define site/solute interactions, derived a similar Gaussian-like statistical function that is regarded as a log-normal distribution of a variable that defines the relative affinity of a solute for a solid phase.

The isotherm, referred to as Modified Freundlich, can be expressed as

$$\frac{S}{S_{\max}} = \frac{K_D C^\beta}{1 + K_D C^\beta}, \quad (4.9)$$

where

S_{\max} = maximum available exchange capacity of solid phase and
 K_D, β = parameters that define the overall solute/solid phase
interaction.

If this isotherm applies, a more comprehensive representation of the heterogeneity of the adsorption is gained from the meaning of K_D and β . These two parameters can be found by regression analysis of a given set of sorption data on the following expression transformed from Equation (4.9):

$$\log \frac{S}{S_{\max} - S} = \beta \log C + \log (K_D^\beta). \quad (4.10)$$

The parameter β has been described (44) as a measure of how sharply peaked, about an average value, is the statistical function for the distribution of surface-binding energies at equilibrium. This parameter has also been described by Crickmore and Wojciechowski (45) as the spread of the statistical function for the distribution of adsorption-desorption rate constants. The parameter K_D has been implicitly related (44) to an average "distribution coefficient," or an average adsorption energy or affinity. Crickmore and Wojciechowski (45), on the other hand, define K_D as the ratio of the reaction rate constants that represent simultaneous β -order adsorption-desorption rates. Both parameters, β and K_D , are temperature and pH dependent.

It is important to note that Equation (4.9) is the general isotherm from which common isotherms can be derived based on the following conditions: Linear isotherms ($\beta = 1$, $K_D^{\beta} C^{\beta} < < 1$), the Langmuir isotherm ($\beta = 1$), and the Freundlich isotherm ($0 < \beta < 1$, $K_D^{\beta} C^{\beta} < < 1$).

4.3.2 Thermodynamics

The thermodynamic parameters used to evaluate sorption mechanisms are the equilibrium constant (K_e), the free energy of sorption (ΔG^0), the enthalpy of sorption (ΔH^0), and the entropy of sorption (ΔS^0). Thus, the equilibrium constant for ion exchange is based on the law of mass action (26) and can be written as

$$K_e = \frac{\bar{a}_A^{z_B} \cdot a_B^{z_A}}{\bar{a}_B^{z_A} \cdot a_A^{z_B}} \quad (4.11)$$

for the reaction



where

A, B = ion species of the binary system in solution,

\bar{A} , \bar{B} = the ion species in the solid phase,

a_A , a_B = the activities of A and B, respectively, in the solution phase,

\bar{a}_A , \bar{a}_B = the activities of A and B, respectively, in the solid phase, and

z_A , z_B = the valences of A and B, respectively.

Equation (4.11) can be expressed in terms of the following modified rational equilibrium constant:

$$K_e = K_r \cdot \frac{\bar{\gamma}_A^{z_B}}{\bar{\gamma}_B^{z_A}} \quad (4.13)$$

$$\text{such that } K_r = \frac{\bar{x}_A^{z_B}}{\bar{x}_B^{z_A}} \cdot \frac{C_B^{z_A}}{C_A^{z_B}} \cdot \frac{\gamma_B^{z_A}}{\gamma_A^{z_B}}, \quad (4.14)$$

where

γ_A, γ_B = the activity coefficients of A and B, respectively, in the solution phase,

$\bar{\gamma}_A, \bar{\gamma}_B$ = the activity coefficients of A and B, respectively, in the solid phase,

C_A, C_B = the molar concentrations of A and B, respectively, in the solution phase, and

\bar{x}_A, \bar{x}_B = the equivalent fractions of A and B, respectively, in the solid phase.

Therefore, the thermodynamic equilibrium constant can be expressed as follows (26):

$$\ln K_e = (z_B - z_A) + \int_0^1 (\ln K_r) d\bar{x}_B, \quad (4.15)$$

where

$$\bar{x}_B = \frac{z_B n_B}{z_A n_A + z_B n_B} \quad (4.16)$$

and

n_A , n_B are moles of A and B, respectively, in the solid phase.

The integral in Equation (4.15) can also be expressed in terms of its components:

$$\begin{aligned} \int_0^1 (\ln K_T) d\bar{x}_B &= z_B \int_0^1 \ln C_A d\bar{x}_B - z_A \int_0^1 \ln C_B d\bar{x}_B \\ &+ z_A \int_0^1 \ln C_B d\bar{x}_B - z_B \int_0^1 \ln C_A d\bar{x}_B + z_A \int_0^1 \ln \gamma_B d\bar{x}_B - z_B \int_0^1 \ln \gamma_A d\bar{x}_B \end{aligned} \quad (4.17)$$

The integral in Equation (4.17) can be solved by several means, for example, graphically or analytically.

The parameters of the Modified Freundlich equation can be substituted into Equation (4.17) and the thermodynamic equilibrium constant may be evaluated, if the components of the Modified Freundlich equation are converted into the same units as those of Equation (4.17).

The Gibbs free energy of sorption ΔG^0 can be determined from the thermodynamic equilibrium constant (45) through the equation

$$\Delta G^0 = -RT \ln K_e, \quad (4.18)$$

where R is the gas constant and T is the absolute temperature.

The enthalpy of sorption can be determined from the van't Hoff equation (18, p. 348)

$$\frac{d \ln K_e}{dT} = \frac{\Delta H^0}{RT^2}. \quad (4.19)$$

Integration of Equation (4.19), with respect to temperature, gives

$$\Delta H^0 = \ln (K_{eT2}/K_{eT1}) \cdot R / [(T_2 - T_1)/T_1 T_2] . \quad (4.20)$$

Equation (4.20) indicates that the equilibrium constant must be obtained at two or more temperatures. If the equilibrium constant is obtained at more than two temperatures, then ΔH^0 can be determined from a plot of $\ln K_e$ vs. $\frac{1}{T}$. The slope of the plot is equal to $-\Delta H^0/R$.

The entropy of sorption ΔS^0 can be determined through the relation

$$\Delta G^0 = \Delta H^0 - T\Delta S^0 . \quad (4.21)$$

The thermodynamic equilibrium constant for sorption in which ion exchange is not considered can be expressed as

$$K_o = \frac{\bar{a}_A}{a_A} , \quad (4.22)$$

where

\bar{a}_A , a_A are the activities of A in the solid and solution phases, respectively.

Equation (4.22) can be expressed as

$$K_o = \frac{\bar{\gamma}_A \bar{C}_A}{\gamma_A C_A} , \quad (4.23)$$

where

$\bar{\gamma}_A$, γ_A are the respective activity coefficients of A in the solid and solution phases.

At infinite dilution, $\bar{\gamma}_A$ and γ_A equal unity. Thus the thermodynamic equilibrium constant can be estimated from the values of \bar{C}_A and C_A at infinite dilution. A simpler technique is also available to estimate \bar{C}_A and C_A at infinite dilution and to calculate an overall equilibrium constant between the concentrations in the solid and in solution of the species or compound of concern (46, 47, 48).

4.4 Pre-experimental Geochemical Modeling

The development of geochemical codes to predict chemical equilibria among aqueous, solid, and gaseous components offers a new design tool for investigators of sorption phenomena (49). The purpose of geochemical modeling was fourfold:

- a. to evaluate the effect of lithium bromide addition on the chemical equilibria of major ions, e.g., Ca^{2+} and CO_3^{2-} ;
- b. to predict possible precipitation or dissolution of the major mineral components of the Prow Pass sample and other components that could be present in the field or that could appear as precipitates during experiments;
- c. to predict the effect of pH on the precipitation or dissolution of the major mineral components of the Prow Pass samples; and
- d. to investigate the distribution of the lithium ion among various expected lithium compounds, e.g., LiOH , Li_2CO_3 .

This study has used the geochemical code PHREEQE (50) as an aid in the design of laboratory batch sorption experiments. This code was selected because it is well documented and is in the public domain. The code includes

models for precipitation, dissolution, and adsorption, and is supported by a thermodynamic data base that is easily expanded by the user.

The simulations used the composition of the J-13 well waters and focused on the mineralogical components of the Prow Pass samples and other possible precipitates that could appear during the experiments. The components, in order of composition by weight, were feldspar, quartz, cristobalite, hematite, and montmorillonite. Others were goethite, barite, calcite, analcime, and magnetite.

The results of the simulations at 38°C predict that the addition of LiBr in concentrations up to 2000 $\mu\text{g mL}^{-1}$ lithium does not significantly change the equilibria of the major cations, Ca^{2+} , Mg^{2+} , Na^+ , or the major anions, SO_4^{2-} , CO_3^{2-} , and Cl^- . The addition of LiBr to J-13 well water is not expected to affect the potential precipitation and solubility of Prow Pass and other minerals. Also, added lithium is not expected to show an effect when the pH is varied from 7 to 9.

The evaluation of the distribution of lithium among different species suggests that >99% lithium will be present as the free ion Li^+ between pH 7 and 9 (Table VII). The species studied were LiOH , LiSO_4^- , Li_2SO_4 , LiCl , LiNO_3 , Li_2CO_3 , and LiBr . The equilibrium constants for these species were derived from reported free energy values (18) and were included in the thermodynamic data base of PHREEQE.

The conclusions from these geochemical simulations permitted a decrease in the number of chemical analyses of ions in the experiments. The simulations also supported the use of total lithium as a good measure of Li^+ for lithium adsorption.

TABLE VII
 PREDICTIONS FOR LITHIUM DISTRIBUTION IN PROV PASS AND J-13 WATER
 ADSORPTION EXPERIMENTS AT 38°C (Li = 2000 $\mu\text{g mL}^{-1}$ AS LiBr)

Species	pH 7	Concentration (mole L^{-1}) pH 8	pH 9
Li ⁺	1.4×10^{-1}	1.4×10^{-1}	1.4×10^{-1}
LiOH	6.6×10^{-8}	4.6×10^{-7}	1.4×10^{-6}
LiSO ₄ ⁻	3.3×10^{-5}	3.3×10^{-5}	3.3×10^{-5}
Li ₂ SO ₄	7.0×10^{-7}	7.0×10^{-7}	7.0×10^{-7}
LiCl	1.4×10^{-5}	1.4×10^{-5}	1.4×10^{-5}
LiNO ₃	2.2×10^{-6}	1.1×10^{-5}	1.2×10^{-5}
Li ₂ CO ₃	4.4×10^{-8}	2.9×10^{-7}	8.0×10^{-7}
LiBr	8.4×10^{-4}	8.4×10^{-4}	8.4×10^{-4}

5.0 RESULTS AND DISCUSSION

This section presents the experimental results and their analysis and interpretation. Emphasis is on modeling of the lithium data by isotherms and estimation of thermodynamic constants. These constants--the relative behavior between adsorption and desorption, and potentiometric studies--are used to classify the controlling sorption mechanism as either physical or chemical.

5.1 Kinetics Experiments

The kinetics experiments had two main objectives: first, to determine minimum equilibration times; second, to provide data for (a) evaluating the role of film transfer and internal diffusion and (b) estimating activation energies.

Batch-tube kinetics experiments conducted at 38⁰C provided a first measure of the minimum equilibration time needed for adsorption. Two initial lithium solution concentrations, 5 and 250 $\mu\text{g mL}^{-1}$, were used to estimate an equilibration period. Although equilibrium was reached rapidly (about 2 hours), a 24-hour equilibrium period was selected as a standard for all adsorption equilibrium experiments.

Desorption kinetics was evaluated for each of the above adsorption experiments. The results indicate that most desorption (-75%) occurs within 6 hours, with additional desorption occurring through the 96-hour sampling time.

An analysis of the kinetics data from the controlled reactors has not been performed for this report. The quality and quantity of the kinetics data have not been evaluated for usefulness in estimating rates for film transfer, particulate diffusion, or surface reaction. A general inspection of the data suggests that it may be possible to model adsorption kinetics. However, the lack of sufficient observations during the first 12 hours makes the desorption

data inadequate for modeling of rates. Both adsorption and desorption kinetics data appear to be of better quality for the controlled reactors than for the batch tubes.

5.2 Equilibrium

Two sets of equilibrium experiments were performed at three temperatures (25°C, 38°C, and 45°C; 38°C is the average temperature of the Yucca Mountain aquifer water). One set was performed over an initial concentration range of 1 to 2000 $\mu\text{g mL}^{-1}$ and at a solid-to-liquid ratio of 1:20. The amount adsorbed is based on the difference between the initial concentration and the equilibrium concentration. Because adsorption was low, the difference in concentration was minimal relative to the analytical error of concentration measurements. In order to minimize the effect of the analytical error, the solid-to-liquid ratio was increased to 1:10 (to increase the number of potential adsorption sites per volume of tracer) and the initial concentration range restricted to 1-150 $\mu\text{g mL}^{-1}$ to enhance the difference in concentrations compared with the analytical error of concentration measurement. The other set of experiments was performed over an initial concentration range of 1 to 150 $\mu\text{g mL}^{-1}$ and at a solid-to-liquid ratio of 1:10. These experiments were performed to determine the extent of sorption and to select suitable isotherms that can be applied to transport modeling. Also, thermodynamic parameters were calculated from the sorption data at the three temperatures to help in differentiating between physical and chemical sorption.

5.2.1 Sorption Calculations

The amount of lithium sorbed to the Prow Pass solid from J-13 well water spiked with concentrations of lithium was determined from the difference in

concentration of lithium in the solution before equilibration and that in the solution concentrations after equilibration. Preliminary evaluation of the sorption data shows large variability at the high solution concentrations after equilibration. The variability is attributed to experimental conditions and to the error associated with the analytical data. For example, the difference between the initial concentration of lithium and that after equilibration can be shown to be within the analytical error of the measured concentrations for the experimental conditions $1000 \mu\text{gLi mL}^{-1}$ initial concentration, 20 mL of solution, 1 g tuff, $1120 \mu\text{g Li g}^{-1}$ maximum sorption (CEC), and 3% analytical error. Thus the variability associated with that difference is very large.

A different procedure, used to determine the amount of lithium sorbed, is based on the assumption that the amount of lithium adsorbed is equal to the amount of cations desorbed from the solid. The data obtained by the two procedures are given in Appendix B (Tables B-I through B-III). The values obtained by calculating differences in lithium concentration are higher at low concentrations of lithium than those obtained by calculating the differences in summed cations. Small differences existed between initial and equilibrated concentrations of some of the individual cations. Those differences were well within analytical error; thus large errors could occur. Some calculated differences gave negative values. In those cases a sum of differences in concentrations resulted in a lower summed concentration of desorbed cations. The difference in lithium concentrations was used in the low-concentration

range and the difference in summed cations was used at the high-concentration range for the best estimate of lithium sorbed.

5.2.2 Isotherm Evaluation

The four isotherms, Linear, Langmuir, Freundlich, and Modified Freundlich, were used to model the two sets of equilibrium experiments discussed above. Linear, Langmuir, and Freundlich were used because of their widespread use in modeling sorption and in the coupling of the sorption isotherms to transport models. The fourth isotherm, the Modified Freundlich, was used because of its theoretical implications. Appendix C compiles all the data from the adsorption and desorption experiments used in the fitting of the four isotherms.

The statistical data on the modeling of sorption by the four isotherms indicate that the sorption data based on best estimates give the better index of determination (R^2) and coefficient of variation (CV). All four isotherms gave R^2 of >0.80 . The CV were 55 percent or better. The Freundlich and Modified Freundlich isotherms gave the best R^2 and CV values, with the Freundlich giving slightly better CV values. Detailed statistical and isotherm parameter data are given in the Tables in Appendix D. Figures 1 through 6 show the results of modeling the data with the Modified Freundlich isotherm. The regression of the best estimate data shows the best variability. The modeling analyses indicate that the sorption of lithium can be effectively represented by all four isotherms. However, the analysis of the Modified Freundlich isotherm provides additional information on the prediction of the extent and heterogeneity of sorption. This extent and heterogeneity of sorption provides an insight into the transport of lithium in

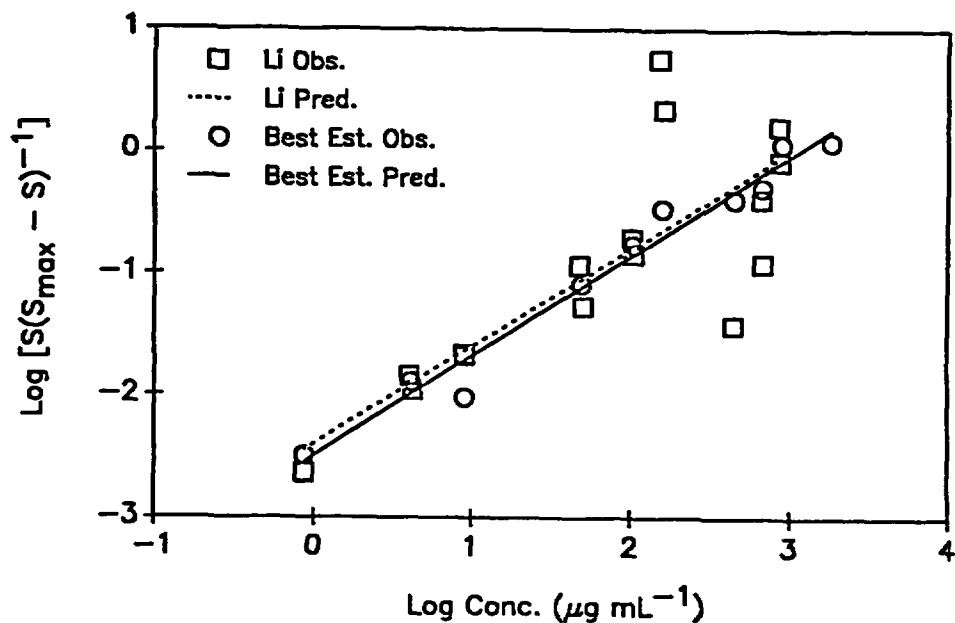


Figure 1. Observed and predicted adsorption of lithium on a Prow Pass suspension in J-13 well water at 25°C for an initial concentration range of 1 to 2000 $\mu\text{g Li mL}^{-1}$ and a solid-to-liquid ratio of 1:20. Adsorbed lithium is determined in two ways: (1) based on measured lithium in solution (Li) and (2) based on a combination of measured lithium and other cations in solution (best estimate). Predicted lithium is based on the Modified Freundlich isotherm.

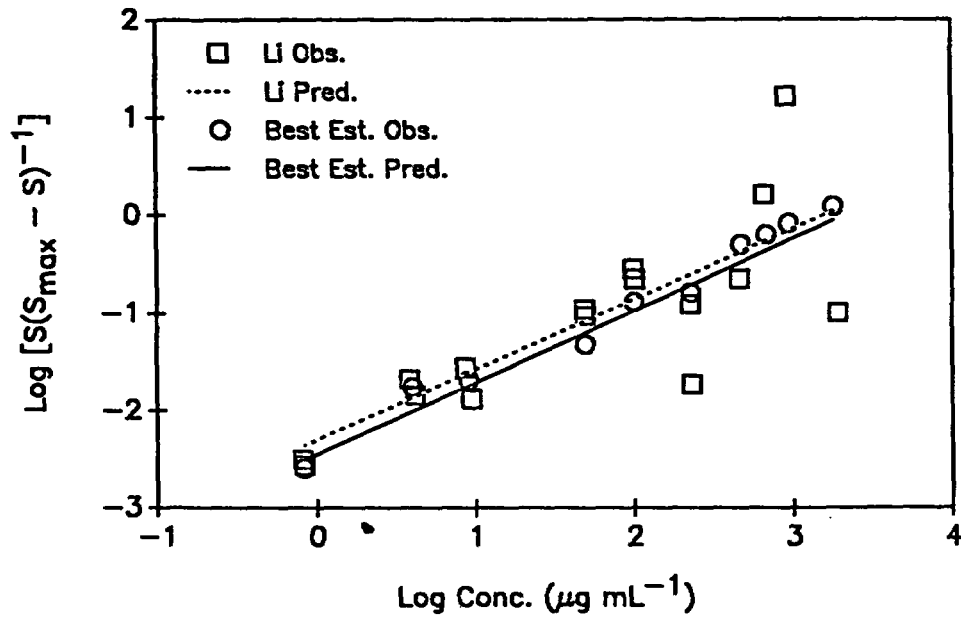


Figure 2. Observed and predicted adsorption of lithium on a Prow Pass suspension in J-13 well water at 38°C for an initial concentration range of 1 to $2000 \mu\text{g Li mL}^{-1}$ and a solid-to-liquid ratio of 1:20. Adsorbed lithium is determined in two ways: (1) based on measured lithium in solution (Li) and (2) based on a combination of measured lithium and other cations in solution (best estimate). Predicted lithium is based on the Modified Freundlich isotherm.

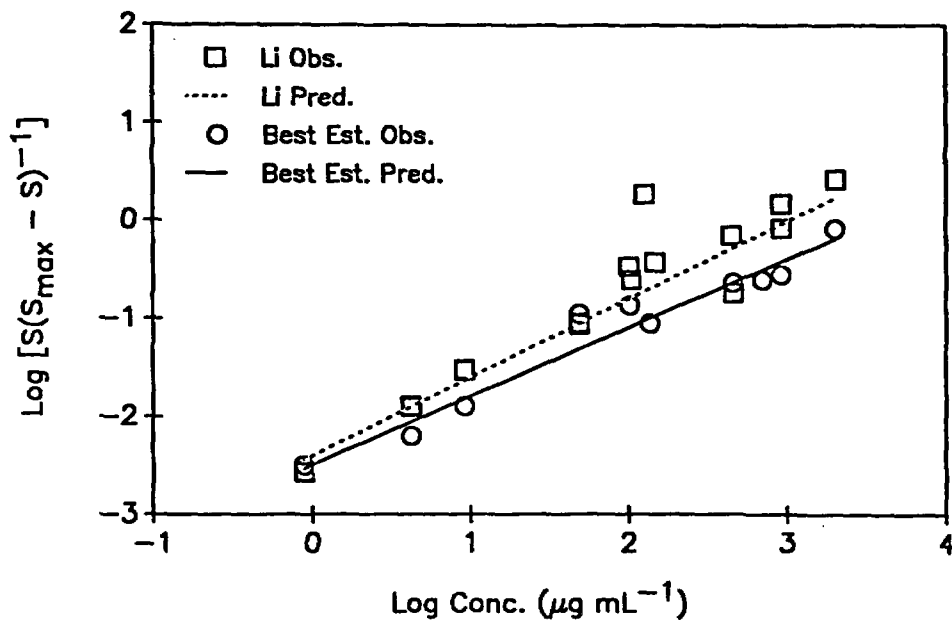


Figure 3. Observed and predicted adsorption of lithium on a Prow Pass suspension in J-13 well water at 45°C for an initial concentration range of 1 to $2000 \mu\text{g Li mL}^{-1}$ and a solid-to-liquid ratio of 1:20. Adsorbed lithium is determined in two ways: (1) based on measured lithium in solution (Li) and (2) based on a combination of measured lithium and other cations in solution (best estimate). Predicted lithium is based on the Modified Freundlich isotherm.

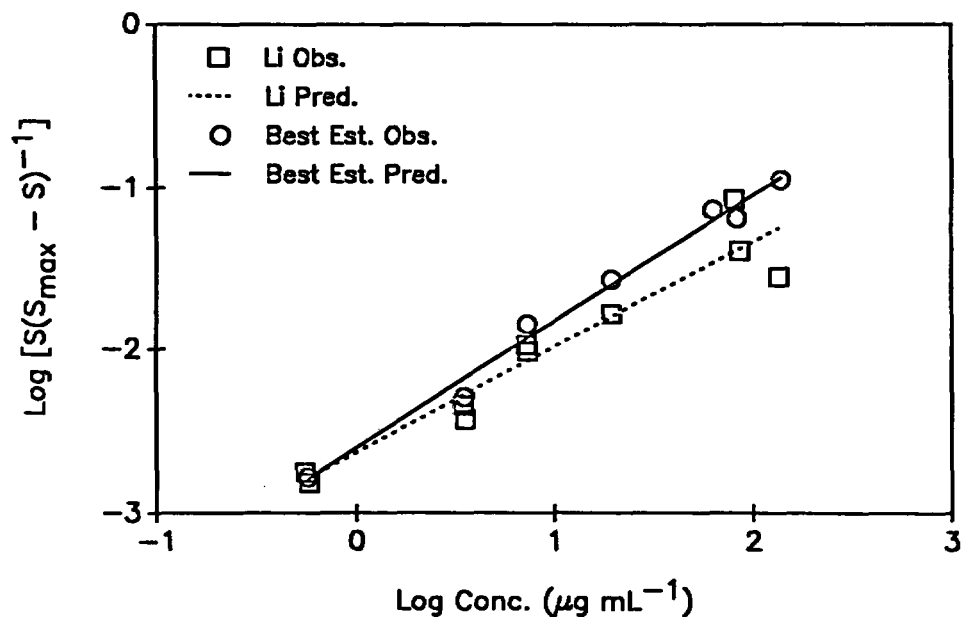


Figure 4. Observed and predicted adsorption of lithium on a Prow Pass suspension in J-13 well water at 25°C for an initial concentration range of 1 to 150 $\mu\text{g Li mL}^{-1}$ and a solid-to-liquid ratio of 1:10. Adsorbed lithium is determined in two ways: (1) based on measured lithium in solution (Li) and (2) based on a combination of measured lithium and other cations in solution (best estimate). Predicted lithium is based on the Modified Freundlich isotherm.

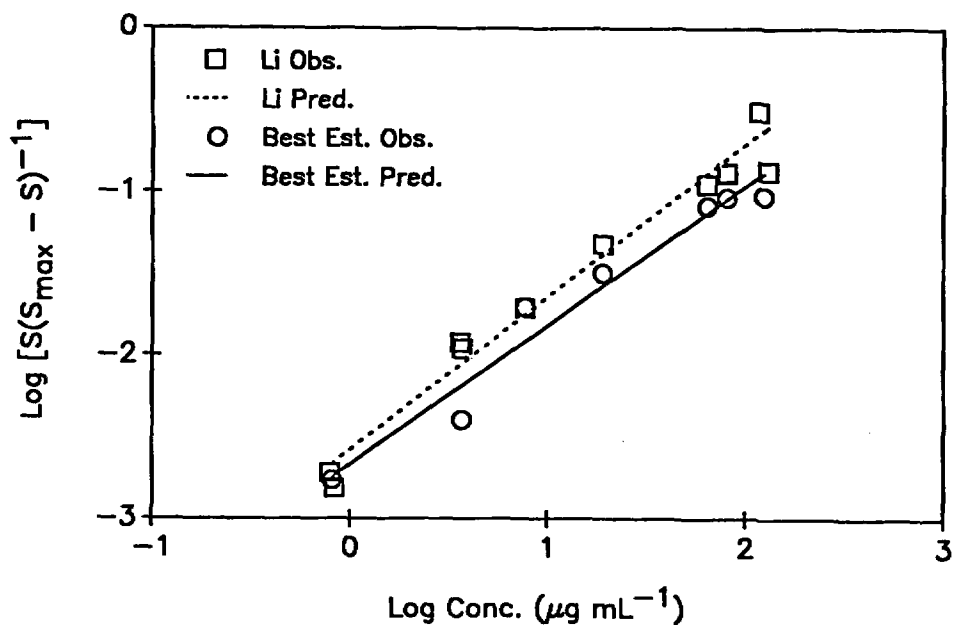


Figure 5. Observed and predicted adsorption of lithium on a Prow Pass suspension in J-13 well water at 38°C for an initial concentration range of 1 to $150 \mu\text{g Li mL}^{-1}$ and a solid-to-liquid ratio of 1:10. Adsorbed lithium is determined in two ways: (1) based on measured lithium in solution (Li) and (2) based on a combination of measured lithium and other cations in solution (best estimate). Predicted lithium is based on the Modified Freundlich isotherm.

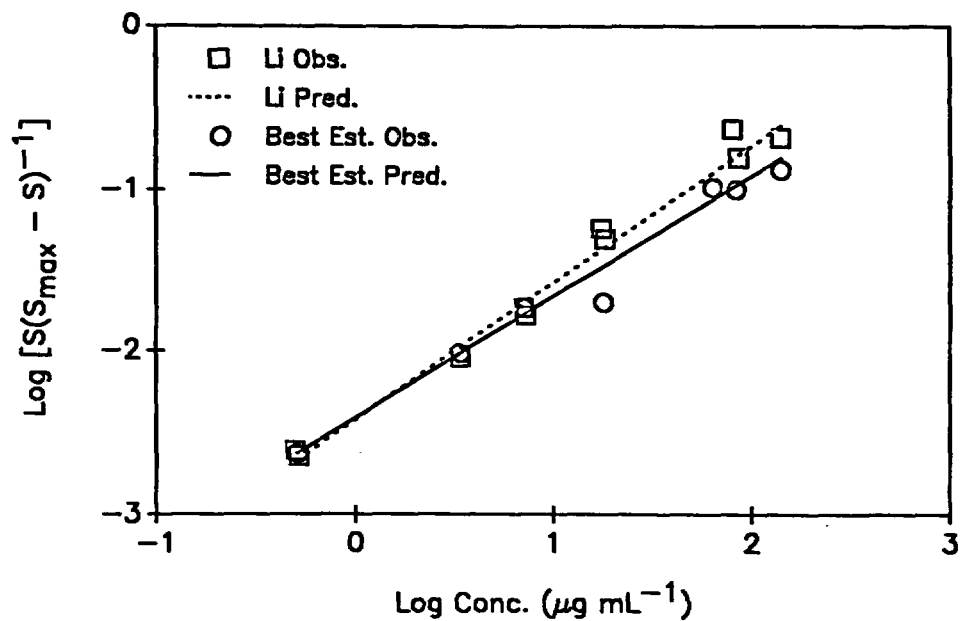


Figure 6. Observed and predicted adsorption of lithium on a Prow Pass suspension in J-13 well water at 45°C for an initial concentration range of 1 to $150 \mu\text{g Li mL}^{-1}$ and a solid-to-liquid ratio of 1:10. Adsorbed lithium is determined in two ways: (1) based on measured lithium in solution (Li) and (2) based on a combination of measured lithium and other cations in solution (best estimate). Predicted lithium is based on the Modified Freundlich isotherm.

laboratory column and field tests. A higher degree of heterogeneity (β -value in the Modified Freundlich isotherm approaches zero) implies that a wider spectrum of retardation factors will occur in transport. This spectrum will have an average extent of retardation as defined by the K_D -value of the same isotherm. Consequently, the following analysis uses the Modified Freundlich isotherm as a reference in predicting the behavior of lithium in transport.

The extent of sorption is related to any of the K parameters of the four models, for example, K in the Freundlich isotherm and k in the Langmuir isotherm. For a better understanding of the relative retardation of lithium predicted by the four isotherms, the retardation parameters were normalized or transformed to those of the linear isotherm, K_d , and the Modified Freundlich isotherm, K_D and β .

The isotherm parameters K_d , K_D , and β are given in Table VIII, along with the transformations. The results indicate that all values of K_d are 2 mL g^{-1} or less; the Langmuir isotherm gives the highest values and the Freundlich gives the lowest values. Retardation can be expressed by the following equation

$$R_f = 1 + \frac{\rho_b K_d}{\theta}, \quad (5.1)$$

where R_f is the retardation factor and is defined as the mean velocity of the moving liquid relative to the mean velocity at which the tracer moves; ρ_b is the dry bulk density of the medium; and θ is the volumetric moisture content. In general, a K_d of 2 or less indicates little sorption-caused retardation of the tracer. Thus lithium appears to be a suitable tracer for the C-wells field test because of low sorptivity.

TABLE VIII
 A COMPARISON OF ESTIMATED PARAMETERS OF FOUR ISOTHERM MODELS FOR THE ADSORPTION OF
 LITHIUM ON A FLOW PASS SUSPENSION IN J-13 WELL WATER FOR AN INITIAL CONCENTRATION
 RANGE OF 1 TO 2000 $\mu\text{g Li mL}^{-1}$ AND A SOLID-TO-LIQUID RATIO OF 1:20

	25°C			38°C			45°C		
	K_d	K_D	β	K_d	K_D	β	K_d	K_D	β
Linear	0.43	3.9×10^{-4}	1.0	0.43	3.9×10^{-4}	1.0	0.27	2.4×10^{-4}	1.0
Langmuir	2.0	2.8×10^{-3}	1.0	1.6	2.3×10^{-3}	1.0	1.2	2.4×10^{-3}	1.0
Freundlich	3.3×10^{-2}	3.0×10^{-5}	0.72	2.0×10^{-2}	1.8×10^{-5}	0.68	1.0×10^{-2}	9.5×10^{-6}	0.65
Modified Freundlich	0.98	8.9×10^{-4}	0.82	0.73	6.6×10^{-4}	0.77	0.33	2.8×10^{-4}	0.70

Transformations:

Linear: $K_d = K_d$

$$K_D = K_d / S_{\max}$$

$$\beta = 1$$

Langmuir: $K_d = kb$

$$K_D = k$$

$$\beta = 1$$

Freundlich: $K_d = \frac{K}{S_{\max}^{1/N}} S_{\max}$

$$K_D = \frac{K}{S_{\max}^{1/N}}$$

$$N = \beta$$

Modified Freundlich: $K_d = K_D S_{\max}$

$$K_D = K_D$$

$$\beta = \beta$$

Based on theoretical considerations, the K_D parameter is a measure of the mean energy sorption of lithium, and the β parameter is a measure of the distribution or spread of individual energies about the mean. Thus under flow conditions, K_D is a measure of the sorption-caused retardation of the tracer and β is a measure of the sorptive dispersion caused by the heterogeneity of sorption; this dispersion is in addition to any hydrodynamic dispersion that may occur. Thus the comparison of K_D and β parameter values in Table VIII for the Linear, Langmuir, and Freundlich isotherms (1 to 2000 $\mu\text{g Li mL}^{-1}$) can be interpreted as follows.

1. The Freundlich isotherm underestimates retardation and overestimates sorptive dispersion.
2. The Langmuir isotherm overestimates retardation and underestimates sorptive dispersion.
3. The Linear isotherm underestimates both retardation and sorptive dispersion.

The effects of overestimation and underestimation can only be inferred from these analyses. Proper statistical discrimination analysis in combination with column experiments is needed to identify the best isotherm under flow conditions.

The statistical and modeling results for the concentration range 1 to 150 $\mu\text{g Li mL}^{-1}$ and a solid-to-liquid ratio of 1:10 are given in Appendix D, Tables D-V through D-IX, for the Linear, Langmuir, Freundlich, and Modified Freundlich isotherms, respectively. The data are based on lithium analysis and best estimates, as was the case in the range 1 to 2000 $\mu\text{g Li mL}^{-1}$. The results indicate that the statistics (R^2 and CV) in general do not differ greatly from the results for the 1-to-2000- $\mu\text{g-Li mL}^{-1}$ data set. Overall, the best-estimate data, as determined from a combination of lithium data and the

summed cation data, can also be represented by the four isotherm expressions. Table IX summarizes the estimated parameters for the four isotherms within this concentration range. The parameters are also expressed in terms of K_d , K_D , and β , in order to compare the expected outcomes of using specific isotherms in transport modeling. As in the case of the 1-to-2000- $\mu\text{g-Li mL}^{-1}$ data set, the interpretation given to these data is as follows.

1. The Freundlich isotherm underestimates retardation and overestimates sorptive dispersion.
2. The Langmuir isotherm overestimates retardation and underestimates sorptive dispersion.
3. The Linear isotherm overestimates retardation and underestimates sorptive dispersion.

A comparison of these results with those of the 1-to-2000- $\mu\text{g-Li mL}^{-1}$ range indicates that in both cases the Freundlich isotherm underestimates retardation and overestimates sorptive dispersion. The Langmuir isotherm model overestimates retardation and underestimates sorptive dispersion for both cases. However, the overestimation of retardation appears significantly greater for the 1-to-150- $\mu\text{g-Li mL}^{-1}$ experiment than for the 1-to-2000- $\mu\text{g-Li mL}^{-1}$ experiment. The Linear isotherm overestimates retardation in the former but underestimates retardation for the latter, even though the amount of overestimation and underestimation appears to be small. Consequently, care should be exercised when selecting an isotherm among several possible alternatives, regardless of their relatively good correlation statistics.

5.2.3 Thermodynamic Parameter Estimation

Thermodynamic parameters were estimated for the lithium sorption of the Provo Pass medium from J-13 well water for the concentration range of 1 to

TABLE IX
 A COMPARISON OF ESTIMATED PARAMETERS OF FOUR ISOOTHERM MODELS FOR THE ADSORPTION OF
 LITHIUM ON A PROW PASS SUSPENSION IN J-13 WELL WATER FOR AN INITIAL
 CONCENTRATION RANGE OF 1 TO 150 $\mu\text{g Li mL}^{-1}$ AND A SOLID-TO-LIQUID RATIO OF 1:10

	25°C			38°C			45°C		
	K_d	K_D	β	K_d	K_D	β	K_d	K_D	β
Linear	0.87	7.9×10^{-4}	1.0	0.96	8.7×10^{-4}	1.0	1.24	1.1×10^{-3}	1.0
Langmuir	2.17	1.3×10^{-2}	1.0	2.06	1.2×10^{-2}	1.0	2.77	1.3×10^{-2}	1.0
Freundlich	3.7×10^{-2}	3.6×10^{-5}	0.759	7.3×10^{-2}	6.6×10^{-5}	0.831	3.7×10^{-2}	3.3×10^{-5}	0.722
Modified Freundlich	0.497	4.5×10^{-4}	0.777	0.806	7.3×10^{-4}	0.852	0.662	6.0×10^{-4}	0.748

Transformations:

Linear: $K_d = K_d$

$K_D = K_d / S_{\max}$

$\beta = 1$

Langmuir: $K_d = kb$

$K_D = k$

$\beta = 1$

Freundlich: $K_d = \left(\frac{K}{S_{\max}}\right)^{1/N} S_{\max}$

$K_D = \left(\frac{K}{S_{\max}}\right)^{1/N}$

$N = \beta$

Modified Freundlich: $K_d = K_d S_{\max}$

$K_D = K_D$

$\beta = \beta$

2000 $\mu\text{g Li mL}^{-1}$ and a solid-to-liquid ratio of 1:20. The assumption in these calculations is that lithium sorption can be modeled as pseudo-binary ion-exchange sorption. During sorption, lithium replaced primarily calcium and sodium ions. Typically, lithium was exchanged with calcium and sodium in an equivalent ratio of 1.6:1 (Ca:Na) in the higher concentration region of lithium and nearly the reverse in the lower concentration region. Therefore, calcium and sodium are considered as a composite ion [ion B in Equation (4.12)] in these calculations. The valence of the composite ion B was estimated as follows.

At high concentrations,

$$z_B = \frac{1.6}{1+1.6} z_{\text{Ca}} + \frac{1}{1+1.6} z_{\text{Na}} = 1.61.$$

At low concentrations,

$$z_B = \frac{1.6}{1+1.6} z_{\text{Na}} + \frac{1}{1+1.6} z_{\text{Ca}} = 1.38.$$

Therefore average z_B is approximately 1.5. The integrated form of Equation (4.18) was used to calculate the thermodynamic equilibrium constant.

$$\begin{aligned} \ln K_e = & (z_B - z_A) - \left(\frac{z_B^\beta - z_B}{\beta} \right) - \left(\frac{z_B - z_A^\beta}{\beta} \right) \\ & + z_A \left(1 + r\bar{\rho} \frac{C_{\text{Bo}}}{C_{\text{Bo}}} \right) \left[\ln \left(\frac{C_{\text{Bo}}}{r\bar{\rho}} + C_{\text{Bo}} \right) - 1 \right] - z_A r\bar{\rho} \frac{C_{\text{Bo}}}{C_{\text{Bo}}} \left[\ln C_{\text{Bo}} - 1 \right] \\ & + z_A \ln \gamma_B - z_B \ln \gamma_A + z_B \ln M_A + z_B \ln K_D, \end{aligned} \quad (5.2)$$

where

z_B = valence of the composite ion B;

z_A = valence of lithium;

β = isotherm parameter;

C_{B0} = the initial concentration of composite ion B adsorbed expressed as $\mu\text{moles B mL}^{-1}$ solid;

C_{B0} = the initial concentration of composite ion B in the solution phase expressed as $\mu\text{moles B mL}^{-1}$ H_2O ;

r = solution-to-solid ratio expressed as $\text{mL H}_2\text{O g}^{-1}$ solid;

$\bar{\rho}$ = solid density expressed as g solid mL^{-1} solid;

$\gamma_B = (\gamma_{Ca} \gamma_{Na})^{1/2}$ = activity coefficient of composite ion B;

γ_A = activity coefficient of lithium in solution phase;

M_A = molecular weight of lithium expressed as $\mu\text{g Li } \mu\text{mole}^{-1}$ Li; and

K_D = isotherm parameter expressed as $\text{mL } \mu\text{g}^{-1}$ Li;

The parameter values used to calculate the thermodynamic equilibrium constants from Equations (4.19) through (4.22) are given in Table X. The estimated values for the equilibrium constants (K_e), Gibb's free energies of sorption (ΔG^0), and enthalpy (ΔH^0) are given in Table XI. The results indicate that the thermodynamic equilibrium constant decreases with an increase in temperature, as does Gibb's free energy of sorption. The enthalpy of sorption between 25°C and 38°C was estimated to be $-5 \text{ kcal mole}^{-1}$. However, the ΔH^0 between 38°C and 45°C was estimated to be about $-36 \text{ kcal mole}^{-1}$. The $-5 \text{ kcal mole}^{-1}$ is more consistent with that expected with lithium, that is, electrostatic or physical sorption. The 7°C difference between 38°C and 45°C is small. Therefore, differences in equilibrium constants will be smaller than when the temperature difference is great. In cases where small

TABLE X
 PARAMETER VALUES FOR THE ESTIMATION OF A THERMODYNAMIC EQUILIBRIUM
 CONSTANT FOR THE LITHIUM ADSORPTION ON A PROX PASS SUSPENSION IN
 J-13 WELL WATER AT THREE TEMPERATURES FOR THE INITIAL CONCENTRATION
 RANGE OF 1 TO 2000 $\mu\text{g Li mL}^{-1}$ AND A SOLID-TO-LIQUID RATIO OF 1:20

	β	K_D	γ_{Li}	γ_{Ca}	γ_{Na}	γ_{B}
25°C	0.823	9.17×10^{-4}	0.978	0.787	0.974	0.876
38°C	0.775	6.90×10^{-4}	0.941	0.783	0.939	0.857
45°C	0.703	2.97×10^{-4}	0.940	0.781	0.938	0.856

$z_A = 1$ $\bar{\rho} = 2.54 \text{ g solid mL}^{-1} \text{ solid}$ $C_{\text{Bo}} = 270.93 \mu\text{mole B mL}^{-1} \text{ solid}$
 $z_B = 1.5$ $r = 20 \text{ mL H}_2\text{O g}^{-1} \text{ solid}$ $C_{\text{Bo}} = 1.798 \mu\text{moles B mL}^{-1} \text{ H}_2\text{O}$
 $M_A = 6.94 \mu\text{g Li mole}^{-1}$
 $M_B = 33 \mu\text{g B } \mu\text{mole}^{-1}$

TABLE XI
 THERMODYNAMIC CONSTANTS ESTIMATED FOR LITHIUM ADSORPTION ON A
 PROV PASS SUSPENSION IN J-13 WELL WATER AT THREE TEMPERATURES
 FOR AN INITIAL CONCENTRATION RANGE OF 1 TO 2000 $\mu\text{g Li mL}^{-1}$
 AND A SOLID-TO-LIQUID RATIO OF 1:20

	25°C	38°C	45°C
K_e	0.001954	0.0013	0.00037
ΔG^0 (kcal mole ⁻¹)	3.7	4.1	5.0
ΔH^0 (kcal mole ⁻¹)	-5.4	-35.5	

differences in equilibrium constants occur, the relative error is expected to increase. Thus, estimated enthalpies (equation 4.20) are subject to more error when temperature differences are small than when they are large. To evaluate the $-36 \text{ kcal mole}^{-1}$ estimate, the enthalpy from the 1-to-150- $\mu\text{g-Li mL}^{-1}$ experiment for 38°C and 45°C was calculated. The experimental design differed in that the solid-to-liquid ratio was 1:10 instead of 1:20. The effective valence of the pseudo-solute B was about 1.2, compared with 1.5 for the first data set. The parameters used in calculating thermodynamic constants are given in Table XII for the 38°C and 45°C data sets. The thermodynamic constants are given in Table XIII. The equilibrium constant value for 38°C is slightly higher than for the first data set (0.0303 compared with 0.0239). This difference can be attributed to differences in the effective valence of the pseudo-ion B. However, the ΔH° estimated for the 38°C and 45°C data is $-5 \text{ kcal mole}^{-1}$, which is the same as that for the 25°C to 38°C data of the 1-to-2000- $\mu\text{g-Li mL}^{-1}$ data set. It should be stated that the method of calculating the enthalpy of sorption is sensitive to the error associated with the estimate of the thermodynamic equilibrium constant. Small errors in the equilibrium constants may result in large differences in enthalpy estimates. For instance, in the case of equation 4.20, errors associated with the natural logarithm of the ratio of the equilibrium constants is multiplied by the large product of two absolute temperatures. Thus, the above conclusions should be kept within the context of the trends from a number of data sets; the average values of enthalpy should not be taken as absolute.

A second approach in estimating the enthalpy of sorption was used to test the above conclusions. The best-estimate data of the 1-to-2000- $\mu\text{m-Li mL}^{-1}$

TABLE XII
 PARAMETER VALUES FOR THE ESTIMATION OF THERMODYNAMIC EQUILIBRIUM CONSTANTS
 FOR LITHIUM ADSORPTION ON A PROX PASS SUSPENSION IN J-13 WELL WATER
 AT 38°C AND 45°C FOR THE INITIAL CONCENTRATION RANGE OF 1 TO 150 $\mu\text{g Li mL}^{-1}$
 AND A SOLID-TO-LIQUID RATIO OF 1:10

	β	K_D	γ_{Li}	γ_{Ca}	γ_{Na}	γ_{B}
38°C	0.852	7.3×10^{-4}	0.978	0.783	0.939	0.857
45°C	0.748	6.0×10^{-4}	0.940	0.781	0.938	0.856

$z_A = 1$	$\bar{\rho} = 2.54 \text{ g solid mL}^{-1} \text{ solid}$
$z_B = 1.2$	$r = 10 \text{ mL H}_2\text{O g}^{-1} \text{ solid}$
$M_A = 6.94 \mu\text{g Li } \mu\text{mole}^{-1}$	$C_{B0} = 270.93 \mu\text{moles B mL}^{-1} \text{ solid}$
$M_B = 27 \mu\text{g B } \mu\text{mole}^{-1}$	$C_{B0} = 1.798 \mu\text{moles B mL}^{-1} \text{ H}_2\text{O}$

TABLE XIII
 THERMODYNAMIC CONSTANTS ESTIMATED FOR LITHIUM
 ADSORPTION ON A PROW PASS SUSPENSION IN J-13 WELL
 WATER AT 38°C AND 45°C FOR AN INITIAL CONCEN-
 TRATION RANGE OF 1 TO 150 $\mu\text{g Li mL}^{-1}$ AND A
 SOLID-TO-LIQUID RATIO OF 1:10

Constant	38°C	45°C
K_e	0.0093	0.0077
ΔG^0 (kcal mole ⁻¹)	2.9	3.1
ΔH^0 (kcal mole ⁻¹)		-5.2

concentration range experiments were used in this approach. The Freundlich equation was used to show the relationship between the concentration of lithium sorbed and the concentration in solution at equilibrium. The parameter values for that equation are given in Appendix D, Table D-III. In this approach the concentration of lithium adsorbed (C_s) is expressed as $\mu\text{g Li mL}^{-1}$ of solution in contact with the surface of the solid. This value can be calculated from the equation (47, 48)

$$C_s = \frac{(\rho/M)A}{S_a/NS}, \quad (5.3)$$

where

ρ is the density of water (g mL^{-1}),

M is the molecular weight of water (g),

A is the cross-sectional area of water ($\text{cm}^2 \text{ molecule}^{-1}$),

N is Avogadro's number,

S_a is the surface area of the solid ($\text{cm}^2 \text{ g}^{-1}$), and

S is the specific adsorption (mg kg^{-1}).

The cross-sectional area of water was calculated from the following equation (46):

$$A = 1.091 \times 10^{-16} [(M \times 10^{24})(N\rho)^{-1}]^{2/3}. \quad (5.4)$$

For the conditions of the lithium experiment, $\rho = 1 \text{ g mL}^{-1}$, $M = 18 \text{ g}$, $A = 105 \times 10^{-15} \text{ cm}^2 \text{ molecule}^{-1}$, $S_a = 34\,600 \text{ cm}^2 \text{ g}^{-1}$, and $N = 6.02 \times 10^{23}$; therefore $C_s = 1015 \times S$.

Equation 5.3 was used to calculate C_s for a series of S values. Also, C_e was calculated for the same S values by inverting the Freundlich isotherm

data. Those results are given in Table XIV. From those data, $\ln (C_s/C_e)$ was plotted against C_s and the curve was extrapolated to $C_s \rightarrow 0$; as $C_s \xrightarrow{\text{lim}} 0$, $(C_s/C_e) = a_s/a_c = K_0$, where K_0 is an equilibrium constant for the sorption process.

The K_0 values obtained from the sorption of lithium at the three temperatures (25°C , 38°C , and 45°C) are given in Table XV, as are average enthalpies calculated with Equation (4.19). The estimated average enthalpies (based on trends) indicate that the mechanism of lithium sorption is physical (electrostatic). The results are consistent with those yielded by the assumption of ion exchange method.

5.2.4 Desorption

The objective of the desorption experiment was to evaluate the reversibility of lithium sorption. Knowledge of the reversibility of lithium sorption will help in determining models for the transport of lithium in the field and in supporting a controlling sorption mechanism of lithium; the electrostatic sorption mechanism is expected to show reversibility.

After the adsorption experiment, the solution was decanted and replaced with J-13 water without lithium. Some lithium remained in solution after decanting. The concentration of lithium in the remaining solution was determined from analysis of an aliquot of the decanted wash solution. J-13 water was equilibrated with the solid containing adsorbed lithium. The solution was then analyzed for lithium and other cations. With the concentration of ions in the adsorbed and solution phases known, the amount of lithium gained in solution was compared with the amount of cations (excluding lithium) lost from solution, and a best estimate was obtained for the amount of lithium sorbed after desorption equilibration. These results, given in

TABLE XIV
 DATA USED IN THE CALCULATION OF EQUILIBRIUM CONSTANTS FOR THE
 ADSORPTION OF LITHIUM ON A PROV PASS SUSPENSION IN J-13 WELL WATER AT
 THREE TEMPERATURES FOR THE INITIAL CONCENTRATION RANGE OF 1 TO 150
 $\mu\text{g Li mL}^{-1}$ AND A SOLID-TO-LIQUID RATIO OF 1:20

S ($\mu\text{g Li g}^{-1}$)	C_s^a ($\mu\text{g Li mL}^{-1}$)	C_e^b ($\mu\text{g Li mL}^{-1}$)		
		25°C	38°C	45°C
4	4.06×10^3	0.96	0.81	1.00
25	2.54×10^4	12.2	12.1	17.0
100	1.02×10^5	83.6	92.7	145
250	2.54×10^5	298	356	598
375	3.81×10^5	522	647	1120
500	5.08×10^5	780	986	1750

$^a C_s$ is calculated by using Equation (5.3).

$^b C_e$ is calculated using its relationship to S as modeled by the Freundlich isotherm (see Section 5.2.3 for the relationship).

TABLE XV
EQUILIBRIUM CONSTANTS AND ENTHALPIES FOR THE ADSORPTION
OF LITHIUM ON A PROX PASS SUSPENSION IN J-13 WELL WATER
AT TEMPERATURES OF 25°C, 38°C, and 45°C FOR THE INITIAL
CONCENTRATION RANGE OF 1 TO 2000 $\mu\text{g Li mL}^{-1}$ AND A
SOLID-TO-LIQUID RATIO OF 1:20

Constant	25°C	38°C	45°C
K_o	7.81	7.85	7.55
ΔH^o (Kcal mole ⁻¹)	0.09 (25°C-38°C)	-0.32 (25°C-45°C)	-1.12 (38°C-45°C)

Figure 7, indicate that desorption data follow the adsorption data in the low concentration range, but in the high concentration range the amount of sorbed lithium is higher for the desorption experiment than for the adsorption experiment. This difference is attributed to the probability that equilibrium was not reached in the desorption experiment because of the high concentration of lithium in solution; that concentration in solution may reduce the rate of outward diffusion.

To further substantiate these conclusions, the desorption data for the 1-to-150- $\mu\text{g-Li mL}^{-1}$ experiment at 38 $^{\circ}\text{C}$ were evaluated similarly. The results, given in Figure 8, indicate that lithium concentrations in the desorption experiment essentially follow those of the adsorption experiment over the range of desorption concentrations. A statistical comparison of the Modified Freundlich isotherms indicates a significant difference in the two regressions at the 95% confidence level, but that difference is attributed to the adsorption data at concentrations higher than those of the desorption data.

The above results indicate that the sorption of lithium is reversible and hysteresis is not evident. The conclusion that lithium sorption is reversible also supports the conclusion drawn from the enthalpy data: physical sorption is the predominant mechanism for the sorption of lithium on the Prow Pass matrix.

5.3 Potentiometric Studies

Potentiometric analysis of mineral surfaces can provide information to permit understanding the mechanisms of sorption exhibited by a solute ion. Data generated by titrating the solid material with potential-determining ions (e.g., H^{+} and OH^{-}) may also be used with models to investigate further the nature of solute interactions with the media (30).

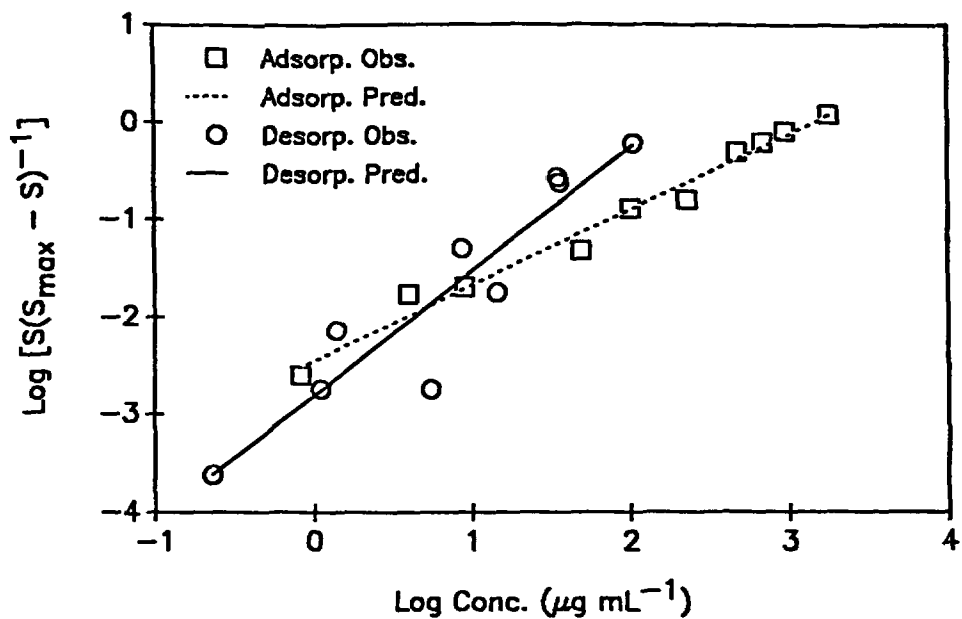


Figure 7. Observed and predicted adsorption and desorption of lithium on a Prow Pass suspension in J-13 well water at 33°C for an initial concentration range of 1 to $2000 \mu\text{g Li mL}^{-1}$ and a solid-to-liquid ratio of 1:20. Predicted lithium is based on the Modified Freundlich isotherm.

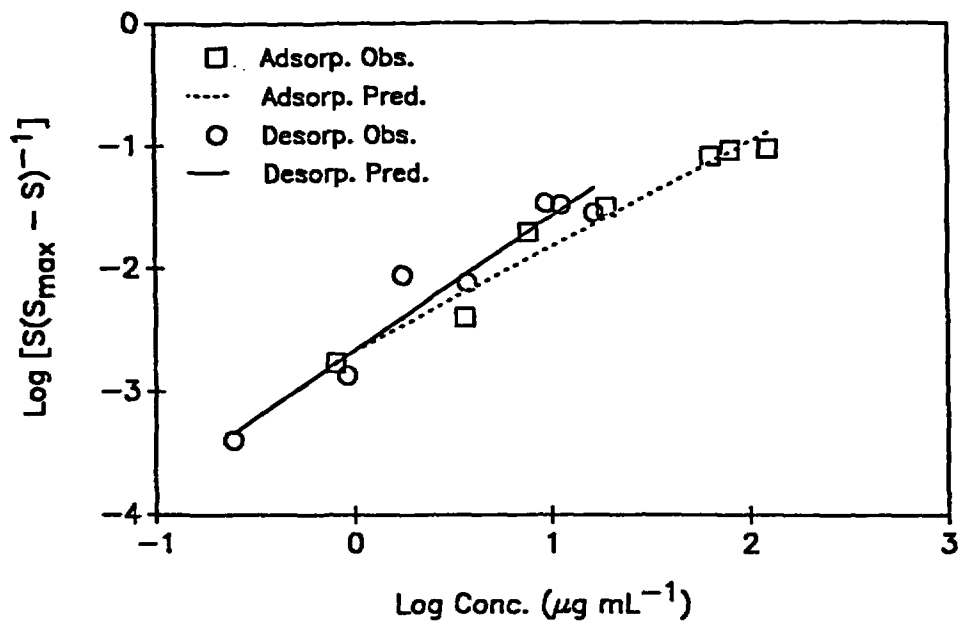


Figure 8. Observed and predicted adsorption and desorption of lithium on a Prox Pass suspension in J-13 well water at 38°C for an initial concentration range of 1 to 150 $\mu\text{g Li mL}^{-1}$ and a solid-to-liquid ratio of 1:10. Predicted lithium is based on the Modified Freundlich isotherm.

Results of the potentiometric titrations are summarized in Figure 9 for no lithium added and Figure 10 for lithium added. All four curves of $s_0 k^{-1}$ plotted against resultant pH show the same pattern. No clear intersections are observed for the two electrolyte concentrations, and the low electrolyte curves are almost always below the high electrolyte curves. The pH at which the two electrolyte concentrations intersect is indicative of the ZPC. The graphs do exhibit a character similar to those reported by other investigators (51) in that the two electrolyte concentrations tend to converge and remain almost indistinguishable below pH 9.

Results of the electrophoresis experiment are summarized in Figures 11 and 12 for the same samples generated in the titration experiment. Whereas the titration measurements were made on the whole sample (<500- μm particle diameter), electrophoresis was measured only on the colloidal fraction (<10- μm diameter). The colloidal fraction may represent the more reactive portion of the sample. EM approached, but did not attain, a zero value. These results support those of the potentiometric titration study.

In all cases, both methods indicated negatively charged particles. The decrease in pH to 2 with the addition of acid was insufficient to neutralize the negative surface charges on the particles. The curves do, however, suggest that a ZPC may occur below pH 2. This finding agrees with published ZPC data (41) for silicates (SiO_2), feldspar, and montmorillonite clay, all of which have ZPCs near or below pH 2. These materials have been identified as the major mineral constituents of the Prow Pass Member (36).

Small amounts of materials with higher ZPC may be present in the sample, but their effect is obscured by the dominance of charges contributed by the

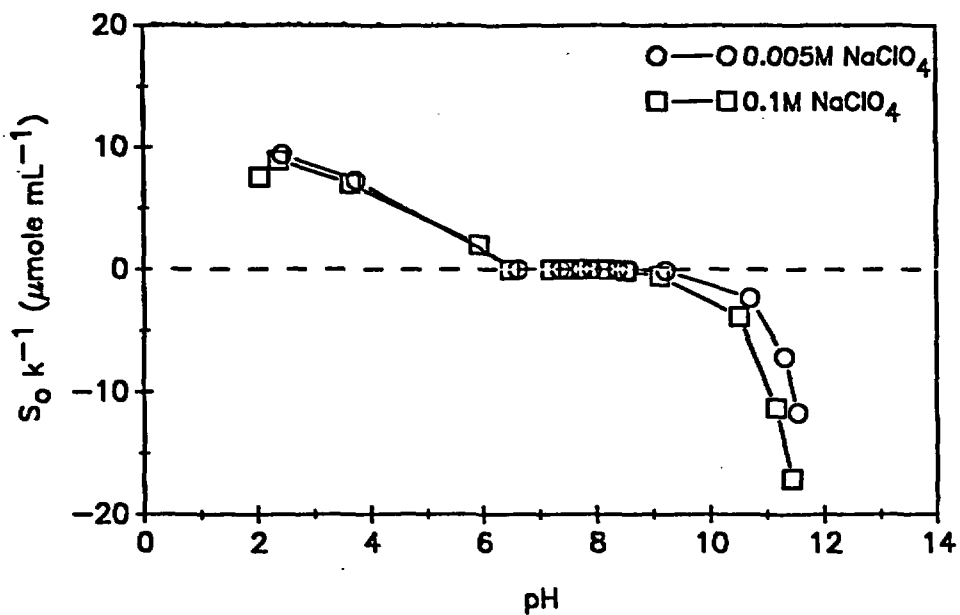


Figure 9. Potentiometric titration of Prow Pass in suspension with J-13 well water and NaClO_4 electrolyte at 38°C without the addition of lithium.

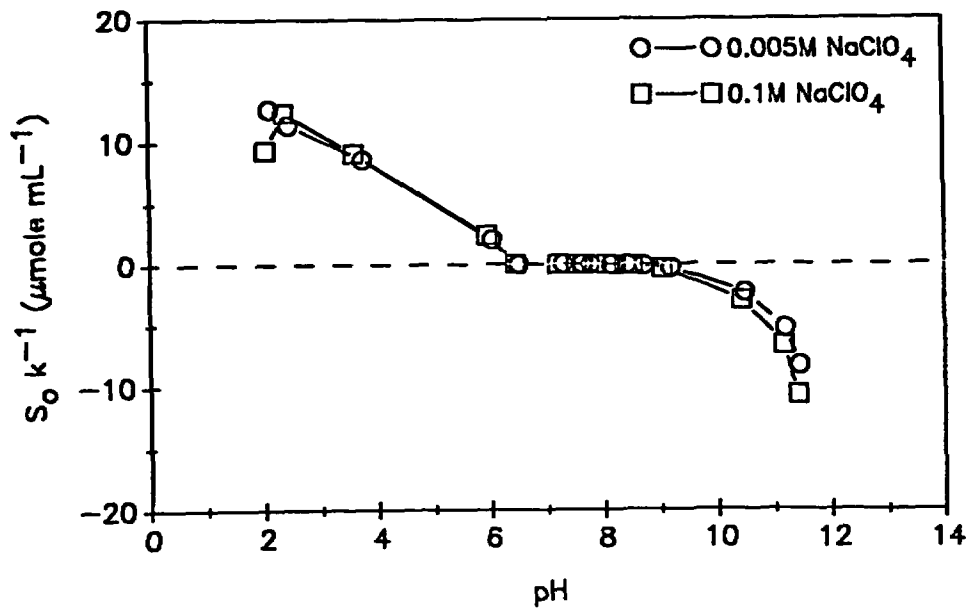


Figure 10. Potentiometric titration of Prow Pass in suspension with J-13 well water and NaClO_4 electrolyte at 38°C with the addition of $900 \mu\text{g Li mL}^{-1}$.

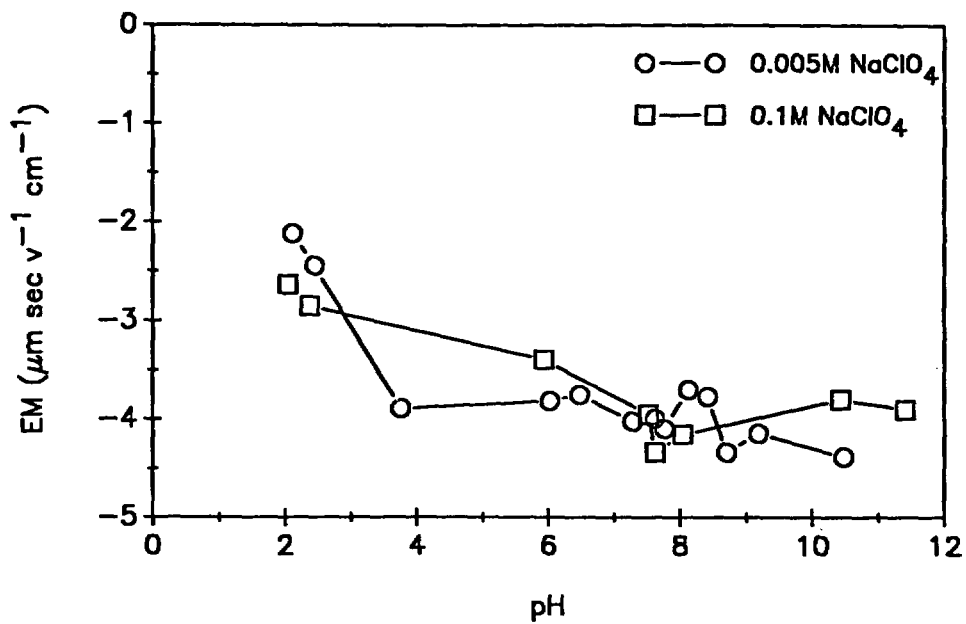


Figure 11. Electrophoretic behavior of a colloidal suspension of Prow Pass in J-13 well water and NaClO₄ electrolyte at 38°C with the addition of 900 $\mu\text{g Li mL}^{-1}$.

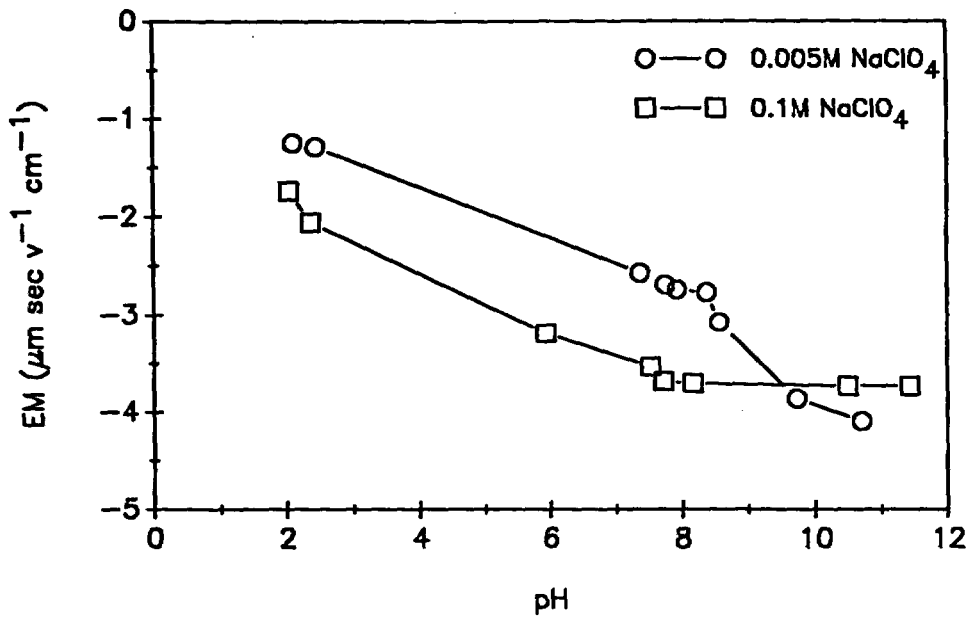


Figure 12. Electrophoretic behavior of a colloidal suspension of Prow Pass in J-13 well water and NaClO_4 electrolyte at 38°C without the addition of lithium.

bulk sample. For example, in natural settings coatings on transmissive fractures or on the bulk materials may be important in defining the sorption mechanisms under hydrologic conditions. The electrophoresis and the titration methods of determining ZPC both indicate the lack of a ZPC between pH 2 and 12 for the Prow Pass material in the presence or absence of added lithium.

6.0 SUMMARY AND CONCLUSIONS

This report includes the results from batch experiments that were conducted to evaluate the potential of lithium, when added as lithium bromide, as a reactive (nonconservative) tracer for tests in the saturated zone of the C-wells subsurface in Yucca Mountain. The main objectives were to model the extent of lithium sorption on Prow Pass suspensions in J-13 well waters and to estimate thermodynamic constants that in combination with potentiometric studies support the classification of lithium sorption either as physical or as chemical.

Lithium (as lithium bromide) was considered a suitable candidate on the basis of the following characteristics: high solubility, good chemical and biological stability, and relatively low sorptivity; no suspicion of bioaccumulation and exclusion as a priority pollutant in pertinent environmental regulations; good analytical detectability and low natural background concentrations; and low cost. Additionally, the literature indicated that retardation by adsorption or by exchange with adsorbers is lower than the retardation of most cations and that its recovery should be reasonably fast (i.e., within the context of the C-wells pump-tracer tests).

Geochemical simulations performed before the experiments with the code PHREEQE suggest that most of the lithium will remain in the form of free lithium with only traces in the form of other species. The simulations also indicate that in a pH range of 7 to 9 neither the stability of the mineral

components of the Prow Pass samples nor the potential for the formation of new precipitates is significantly affected.

Although resource constraints prevented validation of the geochemical code predictions, these simulations support the assumption that lithium analysis is a measure of the lithium cation (Li^+) concentration and thus can be used for estimating concentrations for the isotherm parameters and thermodynamic constants. These simulations also show, within the limitations of the data base and computer code calculations, that precipitation or dissolution did not significantly affect the concentration of lithium in solution. This prediction supports the assumption that the removal of lithium from solution was primarily due to sorption processes.

Biological activity in initial experiments was confirmed by the detection of bacteria and substrates. This occurrence was minimized during subsequent experiments by autoclaving containers and materials before each experiment. Autoclaving was a compromise between having less control of the sorption processes in these experiments and potentially changing the characteristics of the experimental materials.

Abrasion of samples, caused by tumbling or stirring of suspensions, is a concern because of the generation of more sorption area or active sites. The generation of more sorption area or active sites may affect sorption during the performance of batch experiments. Abrasion effects could be important in this study because of the significant, but small, difference between size distributions before and after the contact period. Abrasion has not been shown definitively to be a serious effect because significant differences among replicated representative Prow Pass samples have not been estimated. Nevertheless, this effect is difficult to exclude because of the nature of the batch experiments, so its extent should be characterized.

The equilibrium sorption experimental data indicate that lithium sorption can be modeled by the four isotherms: Linear, Langmuir, Freundlich, and Modified Freundlich. However, theoretical considerations suggest that under flow conditions the four isotherms will predict varied patterns of lithium migration. The Modified Freundlich isotherm is a general isotherm, based on theoretical considerations, and the others are special cases of this general case. Therefore, the Modified Freundlich appears to be the best isotherm for modeling migration of lithium under flow conditions. This conclusion needs to be verified, however, by laboratory column experiments.

Lithium apparently adsorbs to the Prow Pass matrix from J-13 well water by an electrostatic or physical mechanism. Sorption of lithium is easily reversible, a condition consistent with the theory of electrostatic sorption. Also, the enthalpy of sorption appears to be in the range consistent with the enthalpies of physical sorption ($<12 \text{ kcal mole}^{-1}$). Potentiometric and electrophoretic studies were inconclusive because the ZPC could not be determined within the design of the experiments. The electrophoretic results suggest that the ZPC was at a pH less than 2, the lowest pH considered in these experiments.

Some recommendations for future laboratory work are as follows.

1. Expand the temperature and pH range of the experiments for the evaluation of the enthalpy of sorption.
2. Continue to analyze samples from sorption experiments for the tracer of interest and for other constituents that will provide supporting information on the sorption of the tracer.
3. Perform sorption experiments in binary systems as well as in a system of J-13 well water. For example, determine the sorption behavior of lithium in a calcium system and in a sodium system. The

thermodynamics of these systems should permit an extrapolation of results to a system in which both calcium and sodium can control the sorption behavior of lithium (e.g., J-13 well water system).

4. Use additional rock samples as well as representative individual minerals to increase the representativeness of the results for the field tests.
5. Expand the effort to characterize kinetics to improve the understanding of the relative control by physical or chemical sorption processes.
6. Test the ability of the developed isotherms to predict the breakthrough patterns obtained from column studies under various velocities and influent conditions.

The overall conclusion from the laboratory efforts is that lithium bromide is a good candidate tracer for a field test in an environment where the chemistry closely resembles the chemistry of the Prow Pass material in contact with J-13 water and in the presence of dissolved oxygen within a temperature range of 25-45°C and a pH range of about 8. Lithium is expected to be slightly retarded (retardation factor of about 2) with good reversibility. Its adsorption, as suggested by the thermodynamic constants, falls in the category of physical adsorption.

ACKNOWLEDGMENTS

The authors wish to thank Dr. M. Gopala Rao, collaborator from Howard University, for the calculation and interpretation of thermodynamic data. Also, we wish to thank Dr. F. A. Tomei for characterizing the microbial growth

that was observed in our initial experiments. Key contributions have been the analytical chemistry services performed by D. J. Hoard and G. E. Bentley, CLS-1, and the particle size distribution analyses performed by J. Hunter, MST-6. Finally, we thank Sylvia M. Gonzales for her efforts in maintaining the quality assurance documentation and in word processing the manuscript.

REFERENCES

1. Thomas, H. L. 1987. Choose the best catalyst for your reaction. *Research and Development*. 29: 116-119.
2. Cole, D. R. 1983. Theory and application of adsorption and ion exchange reaction kinetics to in situ leaching of ores. *In*: S. S. Augustithis (ed.) *Leaching and diffusion in rocks and their weathering product*. Theophratus Publications S. A., Athens, Greece.
3. Stumm, W., and J. J. Morgan. 1981. *Aquatic chemistry*. John Wiley and Sons, New York, NY.
4. Ruthven, D. M. 1986. *Principles of adsorption and adsorption processes*. John Wiley and Sons, New York.
5. Gaspar, E. (ed.) 1987. *Modern trends in tracer hydrology, Volume I*. CRC Press, Boca Raton, FL.
6. *Handbook of chemistry and physics*. 1973. 54th ed. CRC Press, Cleveland, OH.
7. Sax, N. I. 1984. 6th ed. *Dangerous properties of industrial materials*. Van Nostrand Reinhold Company, New York, NY.
8. Weiss, G. (ed.) 1980. *Hazardous chemicals data book*. Noyes Data Corporation, Park Ridge, NJ.
9. Wedepohl, K. H. 1972. *Handbook of geochemistry, Volume II/1*. Springer Verlag, New York, NY.
10. Wagman, D. D., W. H. Evans, V. B. Parker, R. H. Shumm, and R. L. Nuttal. 1981. Selected values of chemical thermodynamic properties: Compounds of uranium, protactinium, thorium, actinium, and the alkali metals. National Bureau of Standards report TN-270-8.
11. Code of Federal Regulations, Title 40. 1982, 1985. *Protection of environment*. U. S. Government Printing Office, Washington, DC.
12. Mellor, J. W. 1941. *Mellor's comprehensive treatise on inorganic and theoretical chemistry*. Longmans and Green, Co., New York, NY.
13. Sweet, D. V. (ed.) 1987. *Registry of toxic effects of chemical substances*. U. S. Department of Health and Human Services, Cincinnati, OH.
14. Windholz, M. (ed.) 1983. *The Merck index*. Merck and Co., Inc., Rahway, NJ.
15. Bohn, H. L., B. L. McNeal, and G. A. O'Connor. 1979. *Soil chemistry*. John Wiley and Sons, New York, NY.

16. Fortier, J. L., P. A. Leduc and J. E. Desnoyers. 1974. Thermodynamic properties of alkali halides. II. Enthalpies of dilution and heat capacities in water at 25⁰C. *J. Soil Chem.* 3:323-349.
17. Karapet'Yants, M. K., and M. L. Karapet'Yants. 1970. Thermodynamic constants of inorganic and organic compounds. Ann Arbor - Humphrey Science Publishers, Ann Arbor, MI.
18. Garrels, R. M., and C. L. Christ. 1965. Solutions, minerals and equilibria. Harper and Row Publishers, New York, NY.
19. Bear, F. E. 1955. Chemistry of the soil. Reinhold Publishing Corporation, New York, NY.
20. Carmichael, R. S. (ed.) 1982. Handbook of physical properties of rocks. CRC Press, Boca Raton, FL.
21. Bruggenwert, M. G. M. and A. Kamphorst. 1982. Survey of experimental information on cation exchange in soil systems. In: G. H. Bolt (ed.) Soil chemistry, B. physicochemical models. Elsevier Scientific Publishing Co., New York, NY.
22. EA-3356. 1984. Chemical attenuation rates, coefficients, and constants in leachate migration, Volume 2: An annotated bibliography. Electric Power Research Institute, Palo Alto, CA.
23. Gedroiz, K. K. 1922. On the adsorptive power of soils. In: R. D. Harter (ed.) Adsorption phenomena. Van Nostrand Reinhold Soil Science Series, New York, NY.
24. Schachtschabel, P. Von. 1940. Untersuchungen über die sorption der tonmineralien und organischen bodenkolloide, und die bestimmung des anteils dieser kolloide an der sorption in boden. *Kolloid-Beihefte.* 51:199-276.
25. Eisenman, G. 1962. Cation selective glass electrodes and their mode of operation. *Biophysics* 2:259-323.
26. Helfferich, I. 1962. Ion exchange. McGraw-Hill Book Company, Inc., New York, NY.
27. Shainberg, I. and W. D. Kemper. 1967. Ion exchange equilibria on montmorillonite. *Soil Science* 103:4-9.
28. Fuentes, H. R. and W. L. Polzer. 1987. Interpretative analysis of data for solute transport in the unsaturated zone. Los Alamos National Laboratory report NUREG/CR-4737, LA-10817-MS, Los Alamos, NM.
29. Talibudeen, O. 1981. Cation exchange in soils. In: D. J. Greenland and M. H. B. Hayes (eds.). The chemistry of soil processes. Wiley-Interscience, New York, NY.

30. Sposito, G. 1984. The surface chemistry of soils. Oxford University Press, New York, NY.
31. Sittig, M. (ed.) 1980. Priority toxic pollutants. Noyes Data Corporation, Park Ridge, NJ.
32. OTA-0-233. 1984. Protecting the nation's groundwater from contamination. Office of Technology Assessment, Washington, DC.
33. APHA, AWWA, WPCF. 1985. 16th Ed. Standard methods for the examination of water and waste water. American Public Health Association, Washington, DC.
34. ASA, SSSA. 1982. 2nd Ed. Methods of analysis, Part 2. American Society of Agronomy, Inc., Madison, WI.
35. Bish, D. L., D. T. Vaniman, F. M. Byers, Jr., and D. E. Broxton. 1982. Summary of the mineralogy-petrology of tuffs of Yucca Mountain and the secondary-phase thermal stability in tuffs. Los Alamos National Laboratory report LA-9321-MS, Los Alamos, NM.
36. Chipera, S. J. and D. L. Bish. 1988. Mineralogy of drill hole UE-25p#1 at Yucca Mountain, Nevada. Los Alamos National Laboratory report LA-11292-MS, Los Alamos, NM.
37. Memorandum. June 17, 1988. S. J. Chipera and D. L. Bish to G. Lopez. Samples for x-ray analysis. TWS #ESS-1-6/88-15, Los Alamos National Laboratory, Los Alamos, NM.
38. Benson, L. V. and P. W. McKinley. 1985. Chemical composition of ground water in the Yucca Mountain Area, Nevada, 1971-84. U. S. Geological Survey report USGS-DFR-85-484, Denver, CO.
39. Rosin, P. and E. Rammler. 1933. Laws covering the fineness of Powdered Coal. J. Inst. Fuel. 7:29-36.
40. Greenland, D. J. and Hayes, M. H. B. Eds. 1981. The chemistry of soil processes. John Wiley and Sons, New York, NY.
41. Krauskopf, K. B. 1979. Introduction to geochemistry. McGraw-Hill Book Co., New York, NY.
42. Langmuir, I. 1918. The adsorption of gases on plane surfaces of glass, mica and platinum. J. Am. Chem. Soc. 40:1361.
43. Sips, R. 1948. On the structure of a catalyst surface. J. Chem. Phys. 16:490.
44. Sposito, G. 1980. Derivation of the Freundlich equation for ion exchange reactions in soils. Soil Sci. Soc. Am. J. 44:652-654.

45. Crickmore, P. J. and B. W. Wojciechowski. 1977. Kinetics of adsorption of energetically heterogeneous surfaces. *J. Chem. Soc. Faraday Trans.* 173:1216
46. Sparks, D. L. 1986. *Soil physical chemistry*. CRC Press, Boca Raton, FL.
47. Biggar, J. W. and M. W. Cheung. 1973. Adsorption of Picloran (4-amino-3,5,6-trichloropicolinic acid) on Panoche, Ephrata, and Palouse soils: a thermodynamic approach to the adsorption mechanism. *Soil Sci. Soc. Am. J.* 37: 863-868.
48. McCloskey, W. B. and D. E. Bayer. 1987. Thermodynamics of fluridone adsorption and desorption on three California soils. *Soil Sci. Soc. Am. J.* 51: 605-612.
49. EA-3417. 1984. *Geohydrochemical models for solute migration, Volume 1: Process description and computer code selection*. Energy Power Research Institute, Palo Alto, CA.
50. Parkhurst, D. L., D. C. Thorstenson, and L. N. Plummer. 1980. PHREEQE - a computer program for geochemical calculations. U. S. Geological Survey Water, Resources Investigations 80-96.
51. Parker, J. C., L. W. Zelazny, S. Sampath, and W. G. Harris. 1979. A critical evaluation of the extension of zero point of charge (ZPC) theory to soil systems. *Soil Sci. Soc. Amer. J.* 43:668-674.
52. SAS 0-917382-66-8. 1985. *SAS user's guide, statistics, version 5 edition*. SAS Institute, Inc., Cary, NC.

Appendix A
ANALYTICAL INSTRUMENTATION

A variety of analytical instruments have been used in measurements and characterization of either liquid or solid samples. Liquid samples were analyzed on a routine basis by inductively coupled plasma-atomic emission spectroscopy (ICP-AES) for cations with atomic weights less than 80, by inductively coupled plasma-mass spectroscopy (ICP-MS) for cations with atomic weights greater than 80, and by ion chromatography (IC) for anions. The pH of solutions was measured with a Corning pH-Meter Model 130 (expanded pH-range) with an Orion Combination Electrode (precision of ± 0.02 pH units). Characterization of geological samples (Prow Pass cuttings) was accomplished with a Siemens D-500 X-Ray Diffraction System (XRD). Unsuccessful attempts to determine the presence or absence of surface lithium on Prow Pass material were made with a x-ray photoelectron spectroscope (XPS). An alternative approach to determine surface lithium was explored with cylindrical internal reflection-Fourier transform infrared spectroscopy (CIR-FTIR). This effort was discontinued after preliminary results did not prove immediately successful.

Surface area analysis of the Prow Pass samples was performed with a Quantasorb Jr. instrument. The particle size distributions for the same samples were obtained with various instruments: U.S.A. standard testing sieves of stainless steel (W. S. Tyler, Inc.) up to $44 \mu\text{m}$ (mesh 325), and a Micrometric Sedigraph 5000D Particle Size Analyzer for less than $44 \mu\text{m}$ but equal to or greater than $25 \mu\text{m}$.

During the development of experimental procedures the appearance of microbial growth motivated a simple characterization of the growth and organic substrate. Growth was observed by an Olympus microscope (phase contrast and

fluorescence photomicrographs). Bacterial density was estimated by adenosine-triphosphate (ATP) measurements with a Los Alamos Diagnostics Model 535Y Luminometer. Colloidal size distributions were determined with a flow cytometer. Total organic carbon (TOC) analyses were performed on a Photochem total organic analyzer for the determination of organic substrate.

Potentiometric studies comprised titrametric and electrophoretic measurements. Titrametric measurements were made with a combination of a Fisher Burette Model 394, a Fisher Titrate Stirrer Model 385, and a Fisher Electrometer Model 380. Electrophoretic mobility measurements employed a Zeta Meter 3.0 System.

Batch studies used both a modification of a Patterson-Kelley Twin Shell Dry as a rotator (20 rpm) and 500-mL glass resin kettles. Mixing in the kettles was accomplished with paddles turned by G. K. Heller, GT 21-18 Stirrers.

Routine work also employed two Sartorius balances (Model 3704 with a precision of 0.005 g, and Model 3713 with a precision of 0.005/0.05 g), riffle splitters and pulverizers for geological samples, and centrifuges for liquid/solid separation. All experiments, tests, and measurements were conducted in an environmental room with controlled temperature when a constant temperature was required. The room temperature can be maintained to within $\pm 1^{\circ}\text{C}$.

Appendix B

**ESTIMATES OF LITHIUM ADSORPTION
AND DESORPTION EQUILIBRIUM CONCENTRATIONS**

Appendix B is a compilation of data for the adsorption and desorption of lithium on a Prox Pass suspension in J-13 well water at 25°C, 38°C, and 45°C. Given data are based on two methods of evaluating adsorbed and desorbed lithium. Best estimate values are also given and were used in the evaluation of the selection of lithium as a tracer exhibiting physical sorptive properties for the C-wells field tests. Tables B-I through B-III contain adsorption data for experiments performed at an initial concentration range of 1 to 2000 $\mu\text{g Li mL}^{-1}$ and a solid-to-liquid ratio of 1:20. Tables B-IV through B-VI show adsorption data for experiments performed at an initial concentration range of 1 to 150 $\mu\text{g Li mL}^{-1}$ and a solid-to-liquid ratio of 1:10. Table B-VII shows desorption data for those experiments performed at 38°C at an initial concentration range of 1 to 2000 $\mu\text{g Li mL}^{-1}$ and a solid-to-liquid ratio of 1:20. Table B-VIII shows desorption data for those experiments also performed at 38°C but at an initial concentration range of 1 to 150 $\mu\text{g Li mL}^{-1}$ and a solid-to-liquid ratio of 1:10.

TABLE B-I
 ADSORBED LITHIUM CONCENTRATIONS AS ESTIMATED BY TWO METHODS
 AND THOSE CONSIDERED BEST ESTIMATES FOR ADSORPTION ON A PROV PASS
 SUSPENSION IN J-13 WELL WATER AT 25°C FOR AN INITIAL CONCENTRATION
 RANGE OF 1 TO 2000 $\mu\text{g Li mL}^{-1}$ AND A SOLID-TO-LIQUID RATIO OF 1:20

Targeted Initial Concentration ($\mu\text{g Li mL}^{-1}$)	Adsorbed Lithium ($\mu\text{g g}^{-1}$ Solid)		
	Lithium Loss from Solution	Cations Gained in Solution	Best Estimate
1	3.47	0.0	3.47
5	13.9	83.3	13.9
10	198	10.4	10.4
50	83.3	65.9	83.3
100	163	115	163
250	1010	281	392
500	0.0	319	319
750	174	392	392
1000	590	888	590
2000	555	604	604

TABLE B-II
ADSORBED LITHIUM CONCENTRATIONS AS ESTIMATED BY TWO METHODS AND
THOSE CONSIDERED BEST ESTIMATES FOR ADSORPTION ON A PROV PASS
SUSPENSION IN J-13 WELL WATER AT 38°C FOR AN INITIAL CONCENTRATION
RANGE OF 1 TO 2000 $\mu\text{g Li mL}^{-1}$ AND A SOLID-TO-LIQUID RATIO OF 1:20

Targeted Initial Concentration ($\mu\text{g Li mL}^{-1}$)	Adsorbed Lithium ($\mu\text{g g}^{-1}$ Solid)		
	Lithium Loss from Solution	Cations Gained in Solution	Best Estimate
1	2.78	-29.5	2.78
5	18.7	-20.1	18.7
10	21.9	-30.5	21.9
50	101	50.0	50.0
100	221	126	126
250	72.9	153	153
500	10.4	367	367
750	201	423	423
1000	378	494	494
2000	2390	605	605

TABLE B-III
 ADSORBED LITHIUM CONCENTRATIONS AS ESTIMATED BY TWO METHODS
 AND THOSE CONSIDERED BEST ESTIMATES FOR ADSORPTION ON A PROV PASS
 SUSPENSION IN J-13 WELL WATER AT 45°C FOR AN INITIAL CONCENTRATION
 RANGE OF 1 TO 2000 $\mu\text{g Li mL}^{-1}$ AND A SOLID-TO-LIQUID RATIO OF 1:20

Targeted Initial Concentration ($\mu\text{g Li mL}^{-1}$)	Adsorbed Lithium ($\mu\text{g g}^{-1}$ Solid)		
	Lithium Loss from Solution	Cations Gained in Solution	Best Estimate
1	3.47	45.1	3.47
5	13.9	6.94	6.94
10	31.2	13.9	13.9
50	90.2	111	111
100	250	132	132
250	510	90.2	90.2
500	312	208	208
750	729	219	219
1000	590	243	243
2000	1040	500	500

TABLE B-IV
 ADSORBED LITHIUM CONCENTRATIONS AS ESTIMATED BY TWO METHODS
 AND THOSE CONSIDERED BEST ESTIMATES FOR ADSORPTION ON A PROV PASS
 SUSPENSION IN J-13 WELL WATER AT 25°C FOR AN INITIAL CONCENTRATION RANGE
 OF 1 TO 150 $\mu\text{g Li mL}^{-1}$ AND A SOLID-TO-LIQUID RATIO OF 1:10

Targeted Initial Concentration ($\mu\text{g Li mL}^{-1}$)	Adsorbed Lithium ($\mu\text{g g}^{-1}$ Solid)		
	Lithium Loss from Solution	Cations Gained in Solution	Best Estimate
1	1.80	-5.58	1.80
5	4.51	5.60	5.60
10	11.1	15.5	15.5
20	18.0	29.0	29.0
50	-22.0	74.9	75.0
100	64.0	67.0	67.0
150	5.00	111	111

TABLE B-V
 ADSORBED LITHIUM CONCENTRATIONS AS ESTIMATED BY TWO METHODS
 AND THOSE CONSIDERED BEST ESTIMATES FOR ADSORPTION ON A PROW
 PASS SUSPENSION IN J-13 WELL WATER AT 38°C FOR AN INITIAL CONCENTRATION
 RANGE OF 1 TO 150 $\mu\text{g Li mL}^{-1}$ AND A SOLID-TO-LIQUID RATIO OF 1:10

Adsorbed Lithium ($\mu\text{g g}^{-1}$ Solid)			
Targeted Initial Concentration ($\mu\text{g Li mL}^{-1}$)	Lithium Loss from Solution	Cations Gained in Solution	Best Estimate
1	1.90	-4.58	1.90
5	12.5	4.05	4.05
10	21.0	21.2	21.2
20	50.0	33.7	33.7
50	110	83.1	83.0
100	127	92.9	93.0
150	195	94.7	95.0

TABLE B-VI
ADSORBED LITHIUM CONCENTRATIONS AS ESTIMATED BY TWO METHODS
AND THOSE CONSIDERED BEST ESTIMATES FOR ADSORPTION ON A PROV PASS
SUSPENSION IN J-13 WELL WATER AT 45°C FOR AN INITIAL CONCENTRATION RANGE
OF 1 TO 150 $\mu\text{g Li mL}^{-1}$ AND A SOLID-TO-LIQUID RATIO OF 1:10

Targeted Initial Concentration ($\mu\text{g Li mL}^{-1}$)	Adsorbed Lithium ($\mu\text{g g}^{-1}$ Solid)		
	Lithium Loss from Solution	Cations Gained in Solution	Best Estimate
1	2.59	-15.5	2.60
5	10.6	-5.00	10.6
10	19.7	5.11	19.7
20	56.0	21.6	38.8 ¹
50	14.5	103	58.5 ¹
100	175	99.6	137 ¹
150	190	129	160 ¹

¹Values represent the mean of lithium lost and cations gained.

TABLE B-VII
 THE BEST ESTIMATE OF ADSORBED LITHIUM AS DETERMINED BY
 TWO METHODS FOR THE DESORPTION OF LITHIUM FROM A PROV PASS
 SUSPENSION IN J-13 WELL WATER AT 38°C FOR AN INITIAL CONCENTRATION
 RANGE OF 1 TO 2000 $\mu\text{g Li mL}^{-1}$ AND A SOLID-TO-LIQUID RATIO OF 1:20

Targeted Initial Solution Concentration ($\mu\text{g Li mL}^{-1}$)	Lithium Solid Phase Before Desorption ($\mu\text{g g}^{-1}$)	Lithium Gained in Solution (μeq)	Cations ^a Loss From Solution (μeq)	Best Estimate (μeq)	Lithium in Solid Phase after Desorption ($\mu\text{g g}^{-1}$)
1	2.78	0.725	5.47	0.725	0.264
5	18.7	4.82	4.59	4.82	2.00
10	21.9	4.02	10.5	4.02	7.95
50	50.0	16.1	13.9	16.1	2.00
100	126	22.6	20.1	21.3	52.0
250	153	-10.2	38.5	38.5	19.0
500	367	-45.9	45.0	45.0	211
750	423	0.80	54.3	54.3	235
1000	494	-7.53	-11.2	---	---
2000	605	-8.58	54.6	54.6	415

^aExcluding lithium.

TABLE B-VIII
 THE BEST ESTIMATE OF ADSORBED LITHIUM AS DETERMINED BY
 TWO METHODS FOR THE DESORPTION OF LITHIUM FROM A PROV PASS
 SUSPENSION IN J-13 WELL WATER AT 38°C FOR AN INITIAL CONCENTRATION
 RANGE OF 1 TO 150 $\mu\text{g Li mL}^{-1}$ AND A SOLID-TO-LIQUID RATIO OF 1:10

Targeted Initial Solution Concentration ($\mu\text{g Li mL}^{-1}$)	Lithium in Solid Phase Before Desorption ($\mu\text{g g}^{-1}$)	Lithium Gained in Solution (μeq)	Cations ^a Loss From Solution (μeq)	Best Estimate (μeq)	Lithium in Solid Phase After Desorption ($\mu\text{g g}^{-1}$)
1	1.90	0.625	-2.42	0.625	0.45
5	4.41	2.78	1.26	2.78	1.50
10	21.2	5.02	2.74	5.02	9.59
20	33.7	11.0	7.54	11.0	12.3
50	83.1	20.4	20.3	20.3	36.1
100	92.9	24.9	24.8	24.9	35.3
150	94.7	27.7	27.9	27.8	30.5

^aExcluding lithium.

Appendix C
EQUILIBRIUM CONCENTRATIONS AND MODELING VARIABLES

Appendix C compiles all the data sets from the adsorption and desorption equilibrium batch experiments that are referred to in this report. The tables correspond to experiments conducted at 25°C, 38°C, and 45°C for two ranges of initial concentrations of lithium in solution, that is, 1 to 2000 and 1 to 150 $\mu\text{g mL}^{-1}$. Columns labeled S_2 through S_4 and C_2 through C_4 are transformations of equilibrium concentrations C and S used to calculate the linear regressional parameters of the Langmuir, Freundlich, and Modified Freundlich isotherms. The regression of the Linear isotherm uses the C and S values directly. All these variables are inputs to a code based on SAS routines (52) that generates the parameters and the regressional statistics for each isotherm. The various columns are defined as follows:

- C_0 = initial concentration
- CEC = cation exchange capacity of Prow Pass material, $\mu\text{g Li g}^{-1}\text{solid}$
- S = equilibrium concentration on the solid, $\mu\text{g Li g}^{-1}\text{solid}$
- C = equilibrium concentration in solution, $\mu\text{g Li mL}^{-1}\text{H}_2\text{O}$
- S_2 = $C S^{-1}$, dependent variable used in the regression for the Langmuir isotherm
- C_2 = C, independent variable used in the regression for the Langmuir isotherm
- S_3 = $\log S$, dependent variable used in the regression for the Freundlich isotherm
- C_3 = $\log C$, independent variable used in the regression for the Freundlich isotherm
- S_4 = $\log [S(\text{CEC}-S)^{-1}]$, dependent variable used in the regression for the Modified Freundlich isotherm.

$C_4 = \log C$, independent variable used in the regression for the
Modified Freundlich isotherm

Data sets are organized in accordance with the following sequence:

1. Adsorption equilibrium data for the 1-to-2000- $\mu\text{g mL}^{-1}$ range of initial concentrations at a solid-to-liquid ratio of 1:20.
 - 1.1 Temperature = 25 $^{\circ}\text{C}$

Data set based on measured lithium.

Data set based on measured lithium and other cations (best estimate).
 - 1.2 Temperature = 38 $^{\circ}\text{C}$

Data set based on measured lithium.

Data set based on measured lithium and other cations (best estimate).
 - 1.3 Temperature = 45 $^{\circ}\text{C}$

Data set based on measured lithium.

Data set based on measured lithium and other cations (best estimate).
2. Adsorption equilibrium data for the 1-to-150- $\mu\text{g mL}^{-1}$ range of initial concentrations at a solid-to-liquid ratio of 1:10.
 - 2.1 Temperature = 25 $^{\circ}\text{C}$

Data set based on measured lithium.

Data set based on measured lithium and other cations (best estimate).
 - 2.2 Temperature = 38 $^{\circ}\text{C}$

Data set based on measured lithium.

Data set based on measured lithium and other cations (best estimate).

2.3 Temperature = 45°C

Data set based on measured lithium.

Data set based on measured lithium and other cations (best estimate).

3. Desorption equilibrium data at 38°C and a solid-to-liquid ratio of 1:10.

3.1 Data set based on measured lithium and other cations for 1 to 2000 $\mu\text{g mL}^{-1}$.

3.2 Data set based on measured lithium and other cations for 1 to 150 $\mu\text{g mL}^{-1}$.

TABLE C-1

ADSORPTION EQUILIBRIUM DATA FOR THE 1-2000 $\mu\text{g mL}^{-1}$ RANGE OF INITIAL LITHIUM CONCENTRATIONS IN SOLUTION AT 25°C. CONCENTRATIONS CORRESPOND TO MEASURED LITHIUM; SOLID-TO-LIQUID RATIO = 1:20.

C_0	C	CEC	S	C_2	S_2	C_3	S_3	C_4	S_4
1.00	0.87	1104	2.52	0.87	0.3468	-0.05849	0.40140	-0.05849	-2.6406
1.00	0.87	1104	2.58	0.87	0.3376	-0.05998	0.41162	-0.05998	-2.6303
4.86	4.08	1104	15.60	4.08	0.2615	0.61066	1.19312	0.61066	-1.8437
4.86	4.27	1104	11.80	4.27	0.3619	0.63043	1.07188	0.63043	-1.9664
10.20	9.03	1104	23.40	9.03	0.3859	0.95569	1.36922	0.95569	-1.6644
10.20	9.07	1104	22.60	9.07	0.4013	0.95761	1.35411	0.95761	-1.6799
53.50	47.70	1104	116.00	47.70	0.4112	1.67852	2.06446	1.67852	-0.9303
53.50	50.70	1104	56.00	50.70	0.9054	1.70501	1.74819	1.70501	-1.2722
112.00	103.00	1104	180.00	103.00	0.5722	2.01284	2.25527	2.01284	-0.7104
112.00	105.00	1104	140.00	105.00	0.7500	2.02119	2.14613	2.02119	-0.8379
200.00	162.00	1104	760.00	162.00	0.2132	2.20952	2.88081	2.20952	0.3443
200.00	153.00	1104	940.00	153.00	0.1628	2.18469	2.97313	2.18469	0.7583
446.00	444.00	1104	40.00	444.00	11.1000	2.64738	1.60206	2.64738	-1.4249
446.00	461.00	1104	-300.00	461.00	-1.5367	2.66370	.	2.66370	.
682.00	676.00	1104	120.00	676.00	5.6333	2.82995	2.07918	2.82995	-0.9138
682.00	666.00	1104	320.00	666.00	2.0813	2.82347	2.50515	2.82347	-0.3892
895.00	861.00	1104	680.00	861.00	1.2662	2.93500	2.83251	2.93500	0.2051
895.00	870.00	1104	500.00	870.00	1.7400	2.93952	2.69897	2.93952	-0.0821
1844.00	1751.00	1104	1860.00	1751.00	0.9414	3.24329	3.26951	3.24329	.
1844.00	1882.00	1104	-760.00	1882.00	-2.4763	3.27462	.	3.27462	.

TABLE C-11

ADSORPTION EQUILIBRIUM DATA FOR THE 1-2000 $\mu\text{g mL}^{-1}$ RANGE OF INITIAL LITHIUM CONCENTRATIONS IN SOLUTION AT 25°C. CONCENTRATIONS ARE BEST ESTIMATES FROM MEASURED LITHIUM AND OTHER CATIONS; SOLID-TO-LIQUID RATIO = 1:20.

C	S	CEC	C ₂	S ₂	C ₃	S ₃	C ₄	S ₄
0.87	3.47	1104	0.87	0.25072	-0.06048	0.54033	-0.06048	-2.5013
4.18	13.88	1104	4.18	0.30115	0.62118	1.14239	0.62118	-1.8951
9.05	10.41	1104	9.05	0.86936	0.95665	1.01745	0.95665	-2.0214
49.20	83.30	1104	49.20	0.59064	1.69197	1.92065	1.69197	-1.0883
104.00	163.10	1104	104.00	0.63765	2.01703	2.21245	2.01703	-0.7611
158.00	281.00	1104	158.00	0.56228	2.19866	2.44871	2.19866	-0.4667
452.00	319.00	1104	452.00	1.41693	2.65514	2.50379	2.65514	-0.3911
671.00	392.00	1104	671.00	1.71173	2.82672	2.59329	2.82672	-0.2592
895.00	590.00	1104	895.00	1.51695	2.95182	2.77085	2.95182	0.0599
1844.00	604.00	1104	1844.00	3.05298	3.26576	2.78104	3.26576	0.0821

TABLE C-III

ADSORPTION EQUILIBRIUM DATA FOR THE 1-2000 $\mu\text{g mL}^{-1}$ RANGE OF INITIAL LITHIUM CONCENTRATIONS IN SOLUTION AT 38°C. CONCENTRATIONS CORRESPOND TO MEASURED LITHIUM; SOLID-TO-LIQUID RATIO = 1:20.

C_0	C	CEC	S	C_2	S_2	C_3	S_3	C_4	S_4
0.98	0.81	1104	3.40	0.81	0.2382	-0.09151	0.53148	-0.09151	-2.5102
0.98	0.83	1104	3.00	0.83	0.2767	-0.08092	0.47712	-0.08092	-2.5647
4.91	3.80	1104	22.20	3.80	0.1712	0.57978	1.34635	0.57978	-1.6878
4.91	4.14	1104	15.40	4.14	0.2688	0.61700	1.18752	0.61700	-1.8493
10.10	8.63	1104	29.40	8.63	0.2935	0.93601	1.46835	0.93601	-1.5629
10.10	9.39	1104	14.20	9.39	0.6613	0.97267	1.15229	0.97267	-1.8851
53.90	48.50	1104	108.00	48.50	0.4491	1.68574	2.03342	1.68574	-0.9648
53.90	49.20	1104	94.00	49.20	0.5234	1.69197	1.97313	1.69197	-1.0312
111.00	98.90	1104	242.00	98.90	0.4087	1.99520	2.38382	1.99520	-0.5517
111.00	101.00	1104	200.00	101.00	0.5050	2.00432	2.30103	2.00432	-0.6551
230.00	224.00	1104	120.00	224.00	1.8667	2.35025	2.07918	2.35025	-0.9138
230.00	229.00	1104	20.00	229.00	11.4500	2.35984	1.30103	2.35984	-1.7340
470.00	460.00	1104	200.00	460.00	2.3000	2.66276	2.30103	2.66276	-0.6551
470.00	479.00	1104	-180.00	479.00	-2.6611	2.68034	.	2.68034	.
690.00	704.00	1104	-280.00	704.00	-2.5143	2.84757	.	2.84757	.
690.00	656.00	1104	680.00	656.00	0.9647	2.81690	2.83251	2.81690	0.2051
959.00	973.00	1104	-280.00	973.00	-3.4750	2.98811	.	2.98811	.
959.00	907.00	1104	1040.00	907.00	0.8721	2.95761	3.01703	2.95761	1.2109
1915.00	1910.00	1104	100.00	1910.00	19.1000	3.28103	2.00000	3.28103	-1.0017
1915.00	1680.00	1104	4700.00	1680.00	0.3574	3.22531	3.67210	3.22531	.

TABLE C-IV

ADSORPTION EQUILIBRIUM DATA FOR THE 1-2000 $\mu\text{g mL}^{-1}$ RANGE OF INITIAL LITHIUM CONCENTRATIONS IN SOLUTION AT 38°C. CONCENTRATIONS ARE BEST ESTIMATES FROM MEASURED LITHIUM AND OTHER CATIONS; SOLID-TO-LIQUID RATIO = 1:20.

C	S	CEC	C ₂	S ₂	C ₃	S ₃	C ₄	S ₄
0.82	2.78	1104	0.82	0.29496	-0.08619	0.44404	-0.08619	-2.5978
3.97	18.70	1104	3.97	0.21230	0.59879	1.27184	0.59879	-1.7637
9.00	21.90	1104	9.00	0.41096	0.95424	1.34044	0.95424	-1.6938
48.90	50.00	1104	48.90	0.97800	1.68931	1.69897	1.68931	-1.3239
100.00	126.00	1104	100.00	0.79365	2.00000	2.10037	2.00000	-0.8900
226.00	153.00	1104	226.00	1.47712	2.35411	2.18469	2.35411	-0.7935
470.00	367.00	1104	470.00	1.28065	2.67210	2.56467	2.67210	-0.3028
680.00	423.00	1104	680.00	1.60757	2.83251	2.62634	2.83251	-0.2068
940.00	494.00	1104	940.00	1.90283	2.97313	2.69373	2.97313	-0.0916
1795.00	605.00	1104	1795.00	2.96694	3.25406	2.78176	3.25406	0.0837

J

TABLE C-V

ADSORPTION EQUILIBRIUM DATA FOR THE 1-2000 $\mu\text{g mL}^{-1}$ RANGE OF INITIAL LITHIUM CONCENTRATIONS IN SOLUTION AT 45°C. CONCENTRATIONS CORRESPOND TO MEASURED LITHIUM; SOLID-TO-LIQUID RATIO = 1:20.

C_0	C	CEC	S	C_2	S_2	C_3	S_3	C_4	S_4
1.03	0.88	1104	2.96	0.88	0.2977	-0.05458	0.47159	-0.05458	-2.5702
1.03	0.88	1104	3.00	0.88	0.2931	-0.05557	0.47741	-0.05557	-2.5644
4.89	4.21	1104	13.60	4.21	0.3096	0.62428	1.13354	0.62428	-1.9040
4.89	4.19	1104	14.00	4.19	0.2993	0.62221	1.14613	0.62221	-1.8913
10.80	9.21	1104	31.80	9.21	0.2896	0.96426	1.50243	0.96426	-1.5278
10.80	9.18	1104	32.40	9.18	0.2833	0.96284	1.51055	0.96284	-1.5195
53.40	49.00	1104	88.00	49.00	0.5568	1.69020	1.94448	1.69020	-1.0624
53.40	48.80	1104	92.00	48.80	0.5304	1.68842	1.96379	1.68842	-1.0414
115.00	101.00	1104	280.00	101.00	0.3607	2.00432	2.44716	2.00432	-0.4688
115.00	104.00	1104	220.00	104.00	0.4727	2.01703	2.34242	2.01703	-0.6040
162.00	126.00	1104	720.00	126.00	0.1750	2.10037	2.85733	2.10037	0.2730
162.00	147.00	1104	300.00	147.00	0.4900	2.16732	2.47712	2.16732	-0.4281
468.60	445.70	1104	458.00	445.70	0.9731	2.64904	2.66087	2.64904	-0.1494
468.60	460.10	1104	170.00	460.10	2.7065	2.66285	2.23045	2.66285	-0.7399
655.90	699.00	1104	-862.00	699.00	-0.8109	2.84448	.	2.84448	.
655.90	685.00	1104	-582.00	685.00	-1.1770	2.83569	.	2.83569	.
941.40	908.30	1104	662.00	908.30	1.3721	2.95823	2.82086	2.95823	0.1754
941.40	916.20	1104	504.00	916.20	1.8179	2.96199	2.70243	2.96199	-0.0757
2044.00	1974.00	1104	1400.00	1974.00	1.4100	3.29535	3.14613	3.29535	.
2044.00	2004.00	1104	800.00	2004.00	2.5050	3.30190	2.90309	3.30190	0.4202

TABLE C-VI

ADSORPTION EQUILIBRIUM DATA FOR THE 1-2000 $\mu\text{g mL}^{-1}$ RANGE OF INITIAL LITHIUM CONCENTRATIONS IN SOLUTION AT 45°C. CONCENTRATIONS ARE BEST ESTIMATES FROM MEASURED LITHIUM AND OTHER CATIONS; SOLID-TO-LIQUID RATIO = 1:20.

C	S	CEC	C ₂	S ₂	C ₃	S ₃	C ₄	S ₄
0.88	3.47	1104	0.88	0.25360	-0.05552	0.54033	-0.05552	-2.5013
4.20	6.94	1104	4.20	0.60519	0.62325	0.84136	0.62325	-2.1989
9.20	13.90	1104	9.20	0.66187	0.96379	1.14301	0.96379	-1.8945
48.90	111.00	1104	48.90	0.44054	1.68931	2.04532	1.68931	-0.9516
102.50	132.00	1104	102.50	0.77652	2.01072	2.12057	2.01072	-0.8671
136.50	90.20	1104	136.50	1.51330	2.13513	1.95521	2.13513	-1.0507
453.00	208.00	1104	453.00	2.17788	2.65610	2.31806	2.65610	-0.6342
692.00	219.00	1104	692.00	3.15982	2.84011	2.34044	2.84011	-0.6065
912.00	243.00	1104	912.00	3.75309	2.95999	2.38561	2.95999	-0.5494
1989.00	500.00	1104	1989.00	3.97800	3.29863	2.69897	3.29863	-0.0821

TABLE C-VII

ADSORPTION EQUILIBRIUM DATA FOR THE 1-150 $\mu\text{g mL}^{-1}$ RANGE OF INITIAL LITHIUM CONCENTRATIONS IN SOLUTION AT 25°C. CONCENTRATIONS CORRESPOND TO MEASURED LITHIUM; SOLID-TO-LIQUID RATIO = 1:10.

C_0	C	CEC	S	C_2	S_2	C_3	S_3	C_4	S_4
0.744	0.549	1104	1.95	0.549	0.2815	-0.26043	0.29003	-0.26043	-2.7522
0.744	0.575	1104	1.69	0.575	0.3402	-0.24033	0.22789	-0.24033	-2.8144
3.970	3.560	1104	4.10	3.560	0.8683	0.55145	0.61278	0.55145	-2.4286
3.970	3.470	1104	5.00	3.470	0.6940	0.54033	0.69897	0.54033	-2.3420
8.370	7.210	1104	11.60	7.210	0.6216	0.85794	1.06446	0.85794	-1.9739
8.370	7.310	1104	10.60	7.310	0.6896	0.86392	1.02531	0.86392	-2.0135
21.200	19.400	1104	18.00	19.400	1.0778	1.28780	1.25527	1.28780	-1.7806
21.200	19.400	1104	18.00	19.400	1.0778	1.28780	1.25527	1.28780	-1.7806
60.700	62.900	1104	-22.00	62.900	-2.8591	1.79865	.	1.79865	.
60.700	62.900	1104	-22.00	62.900	-2.8591	1.79865	.	1.79865	.
89.600	81.000	1104	86.00	81.000	0.9419	1.90849	1.93450	1.90849	-1.0732
89.600	85.300	1104	43.00	85.300	1.9837	1.93095	1.63347	1.93095	-1.3922
138.000	135.000	1104	30.00	135.000	4.5000	2.13033	1.47712	2.13033	-1.5539
138.000	140.000	1104	-20.00	140.000	-7.0000	2.14613	.	2.14613	.

TABLE C-VIII

ADSORPTION EQUILIBRIUM DATA FOR THE 1-150 $\mu\text{g mL}^{-1}$ RANGE OF INITIAL LITHIUM CONCENTRATIONS IN SOLUTION AT 25°C. CONCENTRATIONS ARE BEST ESTIMATES FROM MEASURED LITHIUM AND OTHER CATIONS; SOLID-TO-LIQUID RATIO = 1:10.

C	S	CEC	C ₂	S ₂	C ₃	S ₃	C ₄	S ₄
0.562	1.82	1104	0.562	0.30879	-0.25026	0.26007	-0.25026	-2.7822
3.520	5.60	1104	3.520	0.62857	0.54654	0.74819	0.54654	-2.2926
7.260	15.50	1104	7.260	0.46839	0.86094	1.19033	0.86094	-1.8465
19.400	29.10	1104	19.400	0.66667	1.28780	1.46389	1.28780	-1.5675
62.900	74.90	1104	62.900	0.83979	1.79865	1.87448	1.79865	-1.1380
83.200	66.90	1104	83.200	1.24365	1.92012	1.82543	1.92012	-1.1904
138.000	111.00	1104	138.000	1.24324	2.13988	2.04532	2.13988	-0.9516

TABLE C-IX

ADSORPTION EQUILIBRIUM DATA FOR THE 1-150 $\mu\text{g mL}^{-1}$ RANGE OF INITIAL LITHIUM CONCENTRATIONS IN SOLUTION AT 38°C. CONCENTRATIONS CORRESPOND TO MEASURED LITHIUM; SOLID-TO-LIQUID RATIO = 1:10.

C_0	C	CEC	S	C_2	S_2	C_3	S_3	C_4	S_4
1.00	0.83	1104	1.7	0.83	0.48824	-0.08092	0.23045	-0.08092	-2.8119
1.00	0.79	1104	2.1	0.79	0.37619	-0.10237	0.32222	-0.10237	-2.7199
4.90	3.60	1104	13.0	3.60	0.27692	0.55630	1.11394	0.55630	-1.9239
4.90	3.70	1104	12.0	3.70	0.30833	0.56820	1.07918	0.56820	-1.9590
9.80	7.70	1104	21.0	7.70	0.36667	0.88649	1.32222	0.88649	-1.7124
9.80	7.70	1104	21.0	7.70	0.36667	0.88649	1.32222	0.88649	-1.7124
24.00	19.00	1104	50.0	19.00	0.38000	1.27875	1.69897	1.27875	-1.3239
24.00	19.00	1104	50.0	19.00	0.38000	1.27875	1.69897	1.27875	-1.3239
75.00	64.00	1104	110.0	64.00	0.58182	1.80618	2.04139	1.80618	-0.9560
75.00	64.00	1104	110.0	64.00	0.58182	1.80618	2.04139	1.80618	-0.9560
93.20	80.60	1104	126.0	80.60	0.63968	1.90634	2.10037	1.90634	-0.8900
93.20	80.40	1104	128.0	80.40	0.62812	1.90526	2.10721	1.90526	-0.8822
143.00	130.00	1104	130.0	130.00	1.00000	2.11394	2.11394	2.11394	-0.8746
143.00	117.00	1104	260.0	117.00	0.45000	2.06819	2.41497	2.06819	-0.5114

TABLE C-X

ADSORPTION EQUILIBRIUM DATA FOR THE 1-150 $\mu\text{g mL}^{-1}$ RANGE OF INITIAL LITHIUM CONCENTRATIONS IN SOLUTION AT 38°C. CONCENTRATIONS ARE BEST ESTIMATES FROM MEASURED LITHIUM AND OTHER CATIONS; SOLID-TO-LIQUID RATIO = 1:10.

C	S	CEC	C ₂	S ₂	C ₃	S ₃	C ₄	S ₄
0.81	1.90	1104	0.810	0.42632	-0.09151	0.27875	-0.09151	-2.7635
3.65	4.40	1104	3.650	0.82955	0.56229	0.64345	0.56229	-2.3978
7.70	21.20	1104	7.700	0.36321	0.88649	1.32634	0.88649	-1.7082
19.00	33.70	1104	19.000	0.56380	1.27875	1.52763	1.27875	-1.5019
64.00	83.10	1104	64.000	0.77016	1.80618	1.91960	1.80618	-1.0894
80.50	92.90	1104	80.500	0.86652	1.90580	1.96802	1.90580	-1.0368
124.00	94.60	1104	124.000	1.31078	2.09342	1.97589	2.09342	-1.0282

TABLE C-XI

ADSORPTION EQUILIBRIUM DATA FOR THE 1-150 $\mu\text{g mL}^{-1}$ RANGE OF INITIAL LITHIUM CONCENTRATIONS IN SOLUTION AT 45°C. CONCENTRATIONS CORRESPOND TO MEASURED LITHIUM; SOLID-TO-LIQUID RATIO = 1:10.

C_0	C	CEC	S	C_2	S_2	C_3	S_3	C_4	S_4
0.77	0.52	1104	2.5	0.52	0.20800	-0.28400	0.39794	-0.28400	-2.6440
0.77	0.50	1104	2.7	0.50	0.18519	-0.30103	0.43136	-0.30103	-2.6105
4.40	3.40	1104	10.0	3.40	0.34000	0.53148	1.00000	0.53148	-2.0390
4.40	3.40	1104	10.0	3.40	0.34000	0.53148	1.00000	0.53148	-2.0390
9.10	7.30	1104	18.0	7.30	0.40556	0.86332	1.25527	0.86332	-1.7806
9.10	7.10	1104	20.0	7.10	0.35500	0.85126	1.30103	0.85126	-1.7340
23.50	17.50	1104	60.0	17.50	0.29167	1.24304	1.77815	1.24304	-1.2405
23.50	18.30	1104	52.0	18.30	0.35192	1.26245	1.71600	1.26245	-1.3060
101.00	80.00	1104	210.0	80.00	0.38095	1.90309	2.32222	1.90309	-0.6291
101.00	86.00	1104	150.0	86.00	0.57333	1.93450	2.17609	1.93450	-0.8035
159.00	140.00	1104	190.0	140.00	0.73684	2.14613	2.27875	2.14613	-0.6822
159.00	140.00	1104	190.0	140.00	0.73684	2.14613	2.27875	2.14613	-0.6822

TABLE C-XII

ADSORPTION EQUILIBRIUM DATA FOR THE 1-150 $\mu\text{g mL}^{-1}$ RANGE OF INITIAL LITHIUM CONCENTRATIONS IN SOLUTION AT 45°C. CONCENTRATIONS ARE BEST ESTIMATES FROM MEASURED LITHIUM AND OTHER CATIONS; SOLID-TO-LIQUID RATIO = 1:10.

C	S	CEC	C ₂	S ₂	C ₃	S ₃	C ₄	S ₄
0.511	2.6	1104	0.511	0.19654	-0.29158	0.41497	-0.29158	-2.6270
3.400	10.6	1104	3.400	0.32075	0.53148	1.02531	0.53148	-2.0135
7.160	19.7	1104	7.160	0.36345	0.85491	1.29447	0.85491	-1.7407
17.900	21.6	1104	17.900	0.82870	1.25285	1.33445	1.25285	-1.6999
63.550	103.0	1104	63.550	0.61699	1.80312	2.01284	1.80312	-0.9876
83.550	100.0	1104	83.550	0.83550	1.92195	2.00000	1.92195	-1.0017
140.000	129.0	1104	140.000	1.08527	2.14613	2.11059	2.14613	-0.8784

TABLE C-XIII

DESORPTION EQUILIBRIUM DATA FOR THE 1-2000 $\mu\text{g mL}^{-1}$ RANGE OF INITIAL LITHIUM CONCENTRATIONS IN SOLUTION AT 38°C. CONCENTRATIONS ARE BEST ESTIMATES FROM MEASURED LITHIUM AND OTHER CATIONS; SOLID-TO-LIQUID RATIO = 1:20.

C	S	CEC	C ₂	S ₂	C ₃	S ₃	C ₄	S ₄
0.23	0.264	1104	0.23	0.87121	-0.63827	-0.57840	-0.63827	-3.6213
1.10	2.000	1104	1.10	0.55000	0.04139	0.30103	0.04139	-2.7412
1.39	7.950	1104	1.39	0.17484	0.14301	0.90037	0.14301	-2.1395
5.48	2.000	1104	5.48	2.74000	0.73878	0.30103	0.73878	-2.7412
8.66	52.100	1104	8.66	0.16622	0.93752	1.71684	0.93752	-1.3051
14.50	19.300	1104	14.50	0.75130	1.16137	1.28556	1.16137	-1.7498
35.80	210.800	1104	35.80	0.16983	1.55388	2.32387	1.55388	-0.6271
34.70	234.720	1104	34.70	0.14784	1.54033	2.37055	1.54033	-0.5686
104.00	415.000	1104	104.00	0.25060	2.01703	2.61805	2.01703	-0.2202

Appendix D

STATISTICAL AND MODEL PARAMETER ESTIMATES FOR ISOTHERMS

TABLE D-I
 STATISTICAL AND MODEL PARAMETER ESTIMATES OF THE LINEAR ISOTHERM FOR THE ADSORPTION OF
 LITHIUM ON A PROW PASS SUSPENSION IN J-13 WELL WATER FOR AN INITIAL CONCENTRATION
 RANGE OF 1 TO 2000 $\mu\text{g Li mL}^{-1}$ AND A SOLID-TO-LIQUID RATIO OF 1:20

	25°C		38°C		45°C	
	Li Data	Best Estimate Data	Li Data	Best Estimate Data	Li Data	Best Estimate Data
R ²	0.18	0.845	0.354	0.905	0.407	0.924
CV	224	55	264	45	188	40
Slope (K _d)	0.35±0.17	0.43±0.06	0.94±0.29	0.425±0.046	0.45±0.12	0.27±0.03

Equation: $S = K_d C$

Regression: S vs C

Units: $S = \mu\text{g Li g}^{-1} \text{ solid}$

$C = \mu\text{g Li mL}^{-1} \text{ H}_2\text{O}$

$K_d = \text{mL H}_2\text{O g}^{-1} \text{ solid}$

TABLE D-II
 STATISTICAL AND MODEL PARAMETER ESTIMATES OF THE LANGMUIR ISOTHERM FOR THE ADSORPTION
 OF LITHIUM ON A PROW PASS SUSPENSION IN J-13 WELL WATER FOR AN INITIAL LITHIUM
 CONCENTRATION RANGE OF 1 TO 2000 $\mu\text{g Li mL}^{-1}$ AND A SOLID-TO-LIQUID RATIO OF 1:20

	25°C		38°C		45°C	
	Li Data	Best Estimate Data	Li Data	Best Estimate Data	Li Data	Best Estimate Data
R ²	0.0004	0.929	0.175	0.888	0.252	0.792
CV	240	22	299	25	127	40
Slope (1/b)	-0.00009 ±0.001	0.001 ±0.0001	0.004 ±0.002	0.0014 ±0.0002	0.0008 ±0.0003	0.0020 ±0.0004
Intercept (1/kb)	1.23±0.80	0.504±0.096	0.013±1.33	0.60±0.12	0.32±0.23	0.85±0.27
b	1.1×10 ⁻⁴	714	2.5×10 ²	714	1.3×10 ³	500
k	7.3×10 ⁻⁵	2.8×10 ⁻³	3.1×10 ⁻¹	2.3×10 ⁻³	2.5×10 ⁻³	2.4×10 ⁻³

Equation: $S = \frac{kbC}{1+kC}$

Regression: C/S vs C

Units: S = $\mu\text{g Li g}^{-1}$ solid

C = $\mu\text{g Li mL}^{-1}$ H₂O

b = $\mu\text{g Li g}^{-1}$ solid

k = mL H₂O μg^{-1} Li

TABLE D-III
 STATISTICAL AND MODEL PARAMETER ESTIMATES OF THE FREUNDLICH ISOTHERM FOR THE
 ADSORPTION OF LITHIUM ON A FLOW PASS SUSPENSION IN J-13 WELL WATER FOR AN INITIAL
 CONCENTRATION RANGE OF 1 TO 2000 $\mu\text{g Li mL}^{-1}$ AND A SOLID-TO-LIQUID RATIO OF 1:20

	25°C		38°C		45°C	
	Li Data	Best Estimate	Li Data	Best Estimate	Li Data	Best Estimate
R ²	0.794	0.963	0.736	0.979	0.926	0.952
CV	21	8.3	24	5.9	11	9.3
Slope (N)	0.72±0.09	0.72±0.09	0.67±0.10	0.68±0.03	0.73±0.05	0.65±0.05
Intercept (log K)	0.65±0.19	0.61±0.11	0.71±0.21	0.66±0.08	0.71±0.11	0.60±0.11

Equation: $S = KC^N$

Regression: log S vs log C

Units: $S = \mu\text{g Li g}^{-1} \text{ solid}$

$C = \mu\text{g Li mL}^{-1} \text{ H}_2\text{O}$

$N = \text{dimensionless}$

$K = (\text{mL } \mu\text{g}^{-1} \text{ Li})^N (\mu\text{g Li g}^{-1} \text{ solid})$

TABLE D-IV
 STATISTICAL AND MODEL PARAMETER ESTIMATES OF THE MODIFIED FREUNDLICH ISOTHERM
 FOR THE ADSORPTION OF LITHIUM ON A PROW PASS SUSPENSION IN J-13 WELL WATER FOR AN
 INITIAL CONCENTRATION RANGE OF 1 TO 2000 $\mu\text{g Li mL}^{-1}$ AND A SOLID-TO-LIQUID RATIO OF 1:20

	25°C		38°C		45°C	
	Li Data	Best Estimate	Li Data	Best Estimate	Li Data	Best Estimate
R^2	0.675	0.973	0.642	0.981	0.909	0.958
CV	56	17	53	13	32	15
Slope (β)	0.80 ± 0.14	0.82 ± 0.05	0.72 ± 0.15	0.77 ± 0.04	0.86 ± 0.07	0.70 ± 0.05
Intercept ($\beta \log K_D$)	-2.4 ± 0.28	-2.50 ± 0.10	-2.3 ± 0.28	-2.45 ± 0.08	-2.4 ± 0.14	-2.49 ± 0.11
K_D	1.0×10^{-3}	8.9×10^{-4}	6.7×10^{-4}	6.6×10^{-4}	1.2×10^{-3}	2.8×10^{-4}

Equation: $S(S_{\max} - S)^{-1} = K_D C$

Regression: $\log [S(S_{\max} - S)^{-1}]$ vs $\log C$

Units: $S = \mu\text{g Li g}^{-1}$ solid

$S_{\max} = \mu\text{g Li g}^{-1}$ solid

$C = \mu\text{g Li mL}^{-1} \text{H}_2\text{O}$

$\beta = \text{dimensionless}$

$K_D = \text{mL H}_2\text{O } \mu\text{g}^{-1} \text{Li}$

TABLE D-V
 STATISTICAL AND MODEL PARAMETER ESTIMATES OF THE LINEAR
 ISOTHERM FOR THE ADSORPTION OF LITHIUM ON A PROX PASS SUSPENSION IN
 J-13 WELL WATER FOR AN INITIAL CONCENTRATION RANGE OF
 1 TO 150 $\mu\text{g mL}^{-1}$ AND A SOLID-TO-LIQUID RATIO OF 1:10

	25°C		38°C		45°C	
	Li Data	Best Estimate	Li Data	Best Estimate	Li Data	Best Estimate
R^2	0.664	0.968	0.970	0.933	0.925	0.957
CV	92	26	26	36	41	31
Slope (K_d)	0.47±0.11	0.87±0.06	1.87±0.09	0.96±0.10	1.58±0.14	1.24±0.11

Equation: $S = K_d C$

Units: $S = \mu\text{g Li g}^{-1} \text{ solid}$

Regression: S vs C

$C = \mu\text{g Li mL}^{-1} \text{ H}_2\text{O}$

$K_d = \text{mL H}_2\text{O g}^{-1} \text{ solid}$

TABLE D-VI
 STATISTICAL AND MODEL PARAMETER ESTIMATES OF THE LANGMUIR ISOTHERM FOR THE ADSORPTION OF
 LITHIUM ON A PROW PASS SUSPENSION IN J-13 WELL WATER FOR AN INITIAL CONCENTRATION
 RANGE OF 1 to 150 $\mu\text{g Li mL}^{-1}$ AND A SOLID-TO-LIQUID RATIO OF 1:10

	25°C		38°C		45°C	
	Li Data	Best Estimate	Li Data	Best Estimate	Li Data	Best Estimate
R ²	0.773	0.843	0.515	0.737	0.839	0.587
CV	50	20	21	25	19	40
Slope (1/b)	0.023±0.004	0.006±0.001	0.0020±0.0007	0.0058±0.0016	0.0030±0.0004	0.0047±0.0017
Intercept (1/kb)	0.44±0.23	0.48±0.08	0.37±0.04	0.48±0.10	0.280±0.028	0.35±0.12
b	43.5	167	500	172	333	213
k	5.2x10 ⁻²	1.3x10 ⁻²	5.4x10 ⁻³	1.2x10 ⁻²	1.1x10 ⁻²	1.3x10 ⁻²

Equation: $S = \frac{k b C}{1 + k C}$

Regression: C/S vs C

Units: S = $\mu\text{g Li g}^{-1}$ solid

C = $\mu\text{g Li mL}^{-1}$ H₂O

b = $\mu\text{g Li g}^{-1}$ solid

k = mL H₂O μg^{-1} Li

TABLE D-VII
 STATISTICAL AND MODEL PARAMETER ESTIMATES OF THE FREUNDLICH ISOTHERM FOR THE
 ADSORPTION OF LITHIUM ON A FLOW PASS SUSPENSION IN J-13 WELL WATER FOR AN INITIAL
 CONCENTRATION RANGE OF 1 to 150 $\mu\text{g Li mL}^{-1}$ AND A SOLID-TO-LIQUID RATIO OF 1:10

	25°C		38°C		45°C	
	Li Data	Best Estimate	Li Data	Best Estimate	Li Data	Best Estimate
R^2	0.924	0.987	0.981	0.958	0.986	0.981
CV	15	6.1	6.6	11	5.9	6.5
Slope (N)	0.638±0.061	0.759±0.039	0.900±0.038	0.831±0.077	0.807±0.031	0.722±0.045
Intercept (K)	0.413±0.077	0.444±0.055	0.477±0.051	0.37±0.11	0.632±0.042	0.643±0.064

Equation: $S = KC^N$

Regression: $\log S$ vs $\log C$

Units: $S = \mu\text{g Li g}^{-1}$ solid

$C = \mu\text{g Li mL}^{-1}$ H_2O

$N =$ dimensionless

$K = (\text{mL } \mu\text{g}^{-1} \text{ Li})^N (\mu\text{g Li g}^{-1} \text{ solid})$

TABLE D-VIII
STATISTICAL AND MODEL PARAMETER ESTIMATES OF THE MODIFIED FREUNDLICH ISOTHERM FOR
THE ADSORPTION OF LITHIUM ON A FROW PASS SUSPENSION IN J-13 WELL WATER FOR AN
INITIAL CONCENTRATION RANGE OF 1 to 150 $\mu\text{g Li mL}^{-1}$ AND A SOLID-TO-LIQUID RATIO OF 1:10

	25°C		38°C		45°C	
	Li Data	Best Estimate	Li Data	Best Estimate	Li Data	Best Estimate
R^2	0.921	0.988	0.982	0.961	0.985	0.979
CV	8.2	4.8	6.6	9.2	6.1	6.9
Slope (β)	0.647±0.063	0.777±0.039	0.936±0.038	0.852±0.077	0.844±0.033	0.748±0.049
Intercept ($\beta \log K_D$)	-2.63±0.079	2.60±0.06	-2.58±0.051	-2.67±0.11	-2.42±0.04	-2.41±0.07
K_D	8.6×10^{-5}	4.5×10^{-4}	1.75×10^{-3}	7.3×10^{-4}	1.35×10^{-3}	6.0×10^{-4}

Equation: $\frac{S}{S_{\max} - S} = K_D C$

Regression: $\log \left(\frac{S}{S_{\max} - S} \right)$ vs $\log C$

Units: $S = \mu\text{g Li g}^{-1} \text{solid}$

$S_{\max} = \mu\text{g Li g}^{-1} \text{solid}$

$C = \mu\text{g Li mL}^{-1} \text{H}_2\text{O}$

$\beta = \text{dimensionless}$

$K_D = \text{mL H}_2\text{O } \mu\text{g}^{-1} \text{Li}$

The following number is for Office of Civilian Radioactive Waste Management (OCRWM) records management purposes only and should not be used when ordering this publication.

Accession Number NNA.890919.0077

This report has been reproduced directly from
the best available copy.

Available to DOE and DOE contractors from
the Office of Scientific and Technical Information
P.O. Box 62
Oak Ridge, TN 37831
prices available from
(615) 576-8401, FTS 626-8401

Available to the public from
the National Technical Information Service
U.S. Department of Commerce
5285 Port Royal Rd.
Springfield, VA 22161

Microfiche A01

<u>Page Range</u>	<u>NTIS Price Code</u>	<u>Page Range</u>	<u>NTIS Price Code</u>	<u>Page Range</u>	<u>NTIS Price Code</u>	<u>Page Range</u>	<u>NTIS Price Code</u>
001-025	A02	151-175	A08	301-325	A14	451-475	A20
026-050	A03	176-200	A09	326-350	A15	476-500	A21
051-075	A04	201-225	A10	351-375	A16	501-525	A22
076-100	A05	226-250	A11	376-400	A17	526-550	A23
101-125	A06	251-275	A12	401-425	A18	551-575	A24
126-150	A07	276-300	A13	426-450	A19	576-600	A25
						601-up*	A99

*Contact NTIS for a price quote.

Los Alamos Los Alamos National Laboratory
Los Alamos, New Mexico 87545